



universität
wien

DIPLOMARBEIT

Titel der Diplomarbeit

„HPK1-mediated negative regulation of T-cell activation -
Characterization of a SLP76-S376A knock-in mouse model“

Verfasser

Victor Navas

angestrebter akademischer Grad

Magister der Naturwissenschaften (Mag.rer.nat.)

Wien, 2012

Studienkennzahl lt. Studienblatt:

A 490

Studienrichtung lt. Studienblatt:

Diplomstudium Molekulare Biologie

Betreuerin / Betreuer:

Univ. Prof. Dr. Timothy Skern

Acknowledgements

I would like to express my gratitude to my master's thesis host lab, for all the support throughout this period.

I am very thankful to have been able to work together with my supervisor, Vincenzo Di Bartolo, whose patience and openness for scientific discussions is truly admirable. Due to my "not yet perfect French" I definitely would have gone lost many times in a jungle of bureaucracy, if it wasn't for Vincenzo and Louise Marie's attentive nature. I sincerely appreciate Céline Cuhe's effort to teach me several techniques, despite my initial confusion, mainly caused by my own "French-deficiency". Furthermore, I want to say thanks to Sonia Aguera Gonzalez and Catherine Inizian for helpful comments during my time as a master student and to Helena Soares for alleviating my pain caused by occasional flow cytometry nightmares with, sometimes direct but very constructive, advice. Of course I want to mention Rémi Lasserre, not only for his kind support with confocal microscopy trouble shooting, but also for his natural positive attitude, which is a real enrichment for the lab's working atmosphere. I had fun times sharing an office with Jérôme Bouchet, whose advice and comments to my work are also truly appreciated. Maria Isabel Thoulouze's excitement during lab meetings often led to high-speed comments, which although often challenging, for me, always were very motivating. I thank her as well for taking time and being open to provide personal advice. Last but not least, I would like to thank our group leader, Andrés Alcover. His relationship with all members of the lab is exemplary, therefore I consider myself lucky to have performed my master's thesis in this lab.

Since, with my graduation an important chapter of my life will be closed, I also want to take the opportunity to sincerely express my deepest gratitude to several key figures outside of Andres's group.

I would like to mention, that I always highly appreciated Magdalena Paolino's, Borries Lubracki's and Max Rössler's guidance during my time as a student. To my mind, Ilka Reichardt, Matt Watson, Roberto Giambruno and Hannah Hochgerner are excellent scientists, whose constant support has been simply invaluable. All these people together with Franziska Stressmann and Ben Steventon have enriched my life scientifically and personally; meanwhile I am lucky to call them friends.

Table of Contents

| | |
|---|-----------|
| Acknowledgements | 1 |
| Table of Contents | 2 |
| | |
| 1. Abstract | 5 |
| | |
| English Version | 5 |
| | |
| 2. Introduction | 6 |
| | |
| 2.1. Overview – T cell development: maturation and differentiation | 6 |
| 2.2. TCR-complex signaling | 10 |
| 2.3. SLP76 | 13 |
| 2.4. The C-terminal SH2 domain of SLP76 binds to ADAP and HPK1 | 14 |
| 2.5. Immunological synapses and organization of signaling complexes | 16 |
| 2.6. Physical and functional interaction between HPK1 and SLP76 | 17 |
| 2.8. Introduction of SLP76-S376A knock-in mouse | 19 |
| 2.9. Aim of this work | 21 |
| | |
| 3. Materials and Methods | 23 |
| | |
| 3.1. Cell culture | 23 |
| 3.1.1. B16-F10 mouse melanoma cell line | 23 |
| 3.1.2. Lewis lung carcinoma | 23 |
| 3.1.3. T8.1 cell line | 24 |
| 3.2. LLC transfection with pGL4.50 [luc2/CMV/Hygro] Vector | 24 |
| 3.2.1. pGL4.50[luc2/CMV/Hygro] Vector | 24 |
| 3.2.2. Transfection of LLC cells using FuGENE® 6 Transfection Reagent | 25 |
| 3.3. Prostaglandin E2 (PGE2) detection | 25 |
| 3.3.1 Procedure and assay principle | 26 |

| | |
|---|----|
| 3.4. Mice | 26 |
| 3.5. CD4+ or CD8+ T-cell purification | 27 |
| 3.6. Activation-induced phosphorylation experiments, using western blot | 27 |
| 3.6.1. T-cell activation using soluble biotin labeled anti mouse CD3 ϵ and CD28 antibodies | 27 |
| 3.6.2. Activation for western blot | 28 |
| 3.6.3. Protein quantification | 29 |
| 3.6.4. Polyacrylamide gel electrophoresis | 29 |
| 3.6.5. Protein transfer to membrane (blotting) | 29 |
| 3.7. Flow cytometry experiments | 31 |
| 3.7.1. Activation-induced phosphorylation experiments, using flow cytometry | 31 |
| 3.7.1.1. T-cell activation for phosphorylation experiments using FCM | 31 |
| 3.7.1.2. Detection of phosphorylation | 32 |
| 3.7.2. Cytokine production assay | 32 |
| 3.7.2.1. Pre-coating 96-well plates for cytokine production assay | 32 |
| 3.7.2.2. Detection of cytokine production | 33 |
| 3.7.3. Proliferation assay | 34 |
| 3.7.3.1. Pre-coating 96-well plates for proliferation assay | 34 |
| 3.7.3.2. Mouse T-cell proliferation assay | 34 |
| 3.7.4. Thymic T-cell development | 35 |
| 3.8. Immunofluorescence and confocal microscopy | 36 |
| 3.8.1. T-cell activation using anti-mouse CD3 ϵ and CD28 antibody-coated coverslips for immunofluorescence | 36 |
| 3.8.1.1. Preparation of antibody coated coverslips | 36 |
| 3.8.1.2. Coating with anti mouse CD3 ϵ and anti mouse CD28 antibodies | 36 |
| 3.8.2. T-cell activation on coverslips pre-coated with anti-mouse CD3 ϵ and anti-mouse CD28 | 37 |
| 3.8.3. Immunofluorescence staining | 38 |
| 3.9. In vivo tumor imaging experiment | 38 |

| | |
|---|-----------|
| 4. Results | 40 |
| 4.1.1. Activation-induced phosphorylation in SLP76-S376A knock-in mouse | 40 |
| 4.1.2. Analysis of SLP76 and ERK phosphorylation by western blotting | 43 |
| 4.2. Cytokine production upon activation of lymph node cells | 46 |
| 4.3. T-cell proliferation assay | 49 |
| 4.4. T-cell development in SLP76-S376A knock-in mice | 52 |
| 4.5. Confocal microscopy experiments to detect possible alterations of microcluster formation in SLP76-S376A mice | 54 |
| 4.6. Set-up of in vivo tumor growth imaging | 56 |
| 5. Discussion | 58 |
| 6. Bibliography | 63 |
| 7. Appendix | 67 |
| Curriculum Vitae | 67 |
| Zusammenfassung (German abstract) | 70 |

1. Abstract

A novel negative regulatory pathway of T-cell activation has been recently described, involving the scaffold protein SRC homology 2 (SH2)-domain-containing leukocyte protein of 76 kDa (SLP76) and the Hematopoietic progenitor kinase 1 (HPK1). It was shown that a single point mutation on SLP76 (S376A) prevents phosphorylation of this protein by HPK1 and impairs the negative regulation of T-cell activation, thus rendering T-cells more sensitive to activating stimuli.

SLP76 is a major component of a signaling platform assembled upon antigen recognition by T-cells. Hence, SLP76 influences various processes including: T-cell survival, proliferation, maturation and differentiation. Furthermore, SLP76 has been reported to be essential for T-cell development.

A SLP76-S376A mutant mouse model has been generated to investigate the physiological consequences of impairing the negative regulatory pathway mentioned above. One of the aims of this Master Thesis was to characterize these SLP76-S376A mutant mice, focusing in particular on the effects of the mutation on early TCR-mediated signaling and downstream effector functions of mature T-cells, as well as on thymic T-cell development,

Our results indicate that SLP76-S376A mice do not exhibit significant defects in T-cell development, in line with previous reports with HPK1 knock-out mice. However, we demonstrated that TCR-stimulation induced higher Extracellular signal-regulated kinases (ERKs) phosphorylation in SLP76-S376A peripheral T-cells compared to wild type cells. Moreover, we observed higher proliferation rates for SLP76-S376A mutant CD4⁺ and CD8⁺ T-cells, as well as increased INF- γ production for SLP76-S376A mutant CD8⁺ T-cells. Collectively, these data suggest that SLP76-S376A mice display a set of altered T-cell properties most likely dependent on a defective negative regulation of TCR-induced signaling.

Recent data demonstrating increased T-cell-dependent anti-tumor immunity in HPK1 knock-out mice (Alzabin et al., 2010), suggest that SLP76-S376A mice may be an optimal tool for investigating whether the negative regulatory function of HPK1 is responsible for its ability to control anti-tumor T-cell responses. Therefore, I also developed and validated a bioluminescent cancer cell line that will be useful to address the importance of the HPK1-SLP76 pathway in anti-tumor immunity.

2. Introduction

2.1. Overview – T cell development: maturation and differentiation

This introduction will present an overview of development and functions of T lymphocytes, focusing in particular on CD4+ and CD8+ T-cells. The aim of this section is to provide a general framework to understand the physiological relevance of the work described in this master thesis. A more detailed description of TCR-dependent signaling pathways and of the particular mutant mouse model used in our studies will be provided in order to understand the scientific questions we asked and the approaches used to address them.

All the cellular elements of blood derive from precursors found in the bone marrow (Figure 1), called hematopoietic stem cells (HSCs). HSCs are pluripotent and give rise to cells with more limited developmental potential called common myeloid progenitor (CMP) and common lymphoid progenitor (CLP). CMPs give rise to red blood cells, platelets and leukocytes of the innate immune system e.g.: mast cells, macrophages and granulocytes. On the other hand, CLPs give rise to B-cells, T-cells and natural killer (NK)-cells. The first two CLP derived cell types belong to the adaptive immune system, whereas NK-cells are classified as innate immune cells. With regard to this work, the focus will be set on immune cells of the adaptive immune system, concentrating particularly on T-lymphocytes.

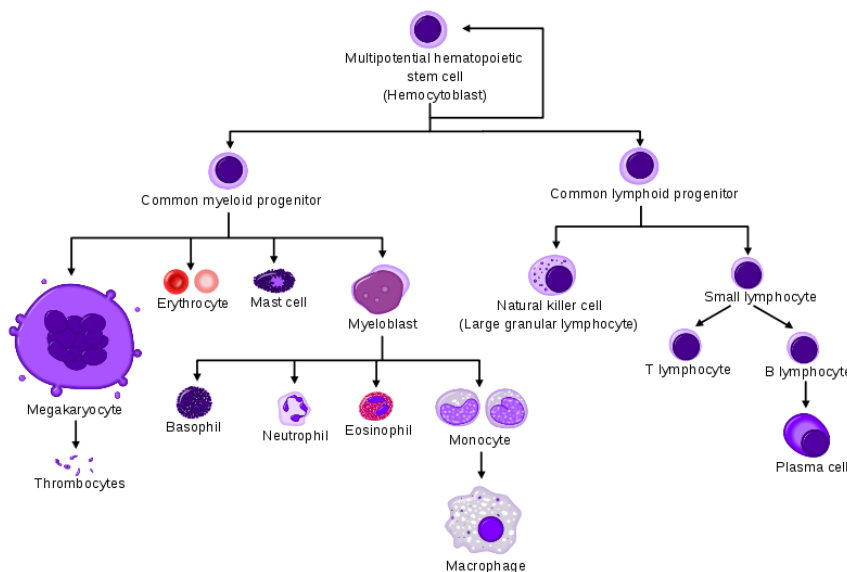


Figure 1

Hematopoiesis.

Hematopoietic stem cells give rise to two major progenitor cell lineages, myeloid and lymphoid progenitors (Regenerative Medicine, 2006)

http://www.allthingsstemcell.com/wp-content/uploads/2010/02/Hematopoiesis_simple_reprogramming1.png

The adaptive immune system is a highly developed network of cells, which recognizes and fights pathogens, toxins or other threats. These potential dangers are identified based on their expression of “non-self antigens”, e.g. elements that are not present in the human body under normal conditions, therefore being unknown to immune cells. In contrast to the innate immune system, the adaptive immune system has the ability to recognize antigens in a highly specific manner. This is achieved by creating high affinity interactions between membrane-bound receptors or soluble proteins (antibodies), expressed by immune cells, and antigens. Another important attribute of the adaptive immune system is the capability of keeping an “immunological memory” of previously encountered antigens, enabling a faster and more efficient response upon secondary infections by the same pathogen.

As mentioned above, T-Lymphocytes develop from CLPs that derive from HSCs. These CLPs have the potential to give rise to either B- or T-Lymphocytes. Whereas, B-cell maturation takes place in the bone marrow, some CLPs get selected to migrate to the thymus. Bone marrow and thymus are referred to as primary or central lymphoid organs and provide a suitable environment for generation and development of lymphocytes. On the other hand, secondary or peripheral lymphoid organs, including lymph nodes, spleen, mucosal lymphoid tissues of the gut, the nasal respiratory tract, the urogenital tract and other mucosa, favor antigen encounter and initiation of immune responses by mature cells. Once CLPs arrive at the thymus, they commit to the T-cell lineage. This commitment is most probably mediated by interactions with thymic stromal cells involving the notch-signaling pathway.

The thymus consists of several lobules. These lobules are structured in two different regions (Figure 2). The cortex (outer region) contains epithelial cells and immature thymocytes surrounded by a subcapsular epithelium and a capsule. The medulla (central region) also contains epithelial cells, as well as macrophages, dendritic cells, Hassal’s corpuscle and mature thymocytes. Hence, thymocytes mature as they migrate deeper into the thymus. The outer cortical cell layer mostly contains proliferating immature lymphocytes, whereas immature cells already undergoing thymic selection are positioned further deep inside the cortex. Eventually, mature T-cells are found in the medulla.

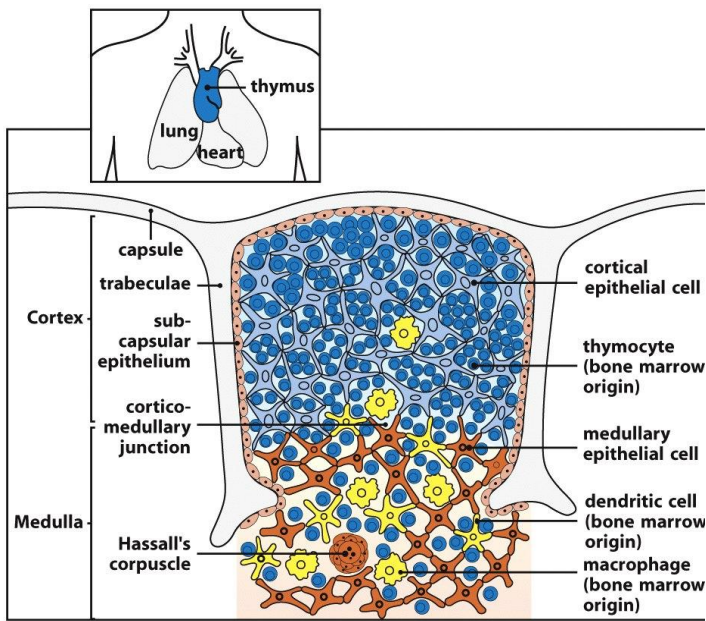


Figure 7-15 Immunobiology, 7ed. (© Garland Science 2008)

Figure 2

The cellular organization of the human thymus. The Thymus is made up of lobules, which contain a cortical (outer) and a medullary (central) region. Cells present in the cortical region: immature thymocytes (dark blue), branched cortical epithelial cells (pale blue), scattered macrophages. Cells present in the medullary regions: mature thymocytes (dark blue), medullary epithelial cells (orange), macrophages and dendritic cells (yellow). (Janeway's Immunobiology, seventh edition).

Once committed to the T-cell lineage (as mentioned above), CLPs start expressing CD2 in humans, or Thy-1 in mice, which are cell surface molecules specific of T-lymphocytes. Four major subsets of immature T cells, distinguishable by their expression of CD4 and CD8 co-receptors, are found in the thymus. Cells expressing neither CD4 nor CD8 are called double negative (DN) and are the most immature, while cells expressing both co-receptors are named double positive (DP). Mature thymocytes express only one co-receptor, hence are defined as CD4+ or CD8+ single positive (SP) cells.

DN cells account for about 5% of all thymocytes. They consist of 60% immature T cells that will express $\alpha:\beta$ TCR restricted to MHC molecules. The remaining DN cells include mature $\gamma:\delta$ T-cells, that do not express co-receptors, and NKT cells, bearing and $\alpha:\beta$ T-cell receptor recognizing CD1 molecules as well as the NK1.1 receptor. $\gamma:\delta$ T-cells are the first to appear in embryonic development and play a role in the gut mucosa and the epithelia of the reproductive tract. However, in the rest of this work we will focus on $\alpha:\beta$ T-cells, which engage with MHC molecules and develop further into single positive T-cells.

DN cells that lack the three markers defining mature T-cells, i.e. the T-cell receptor (TCR)/CD3 complex (see paragraph 1.2. *TCR-complex signaling*), CD4 and CD8 receptors, can be further divided into four subsets named DN1 to DN4. The DN1 sub-population is defined by expression of c-Kit (Stem Cell Factor receptor) and CD44

(an adhesion molecule) but not CD25 (α -chain of IL-2 receptor). At this stage, the genes encoding for the T-cell receptor are in germline configuration. In the DN2 sub-population, both CD44 and CD25 are expressed and rearrangements of the T-cell receptor β -chain locus begin (D_{β} to J_{β} -rearrangement). Further V_{β} to DJ_{β} -rearrangements and down-regulation of CD44 occur in DN3. Only cells, which exhibit productive β -chain rearrangements lose CD25 expression and proceed to DN4 sub-population. The assembly of a CD3:pre T-cell receptor complex (including a rearranged β -chain coupled to a preT α subunit) enables signaling, which triggers proliferation and arrest of further β -chain rearrangements. Shortly thereafter, both co-receptors are expressed CD4 and CD8, thus giving rise to DP T-cells.

Around 5×10^7 new cells are generated every day in the thymus of a healthy mouse. Nevertheless, only 2-4% of these cells exit the thymus as mature T-cells, while the remaining are eliminated during a process called thymic selection (Figure 3). DP thymocytes, that represent the biggest cell population in the thymus, are selected at this stage by their ability to bind to self:peptide-MHC molecular complexes. T-cells, which do not bind die by apoptosis in a process called “death by neglect”. Cells that bind to self:peptide-MHC with too high affinity undergo “negative selection” and get eliminated as well at the DP and/or SP stage. This step prevents the production of cells with potential to create auto immune reactions. Hence, only cells whose TCR engages with self:peptide-MHC complexes with intermediate affinities escape deletion and are "positively selected" and continue their maturation process.

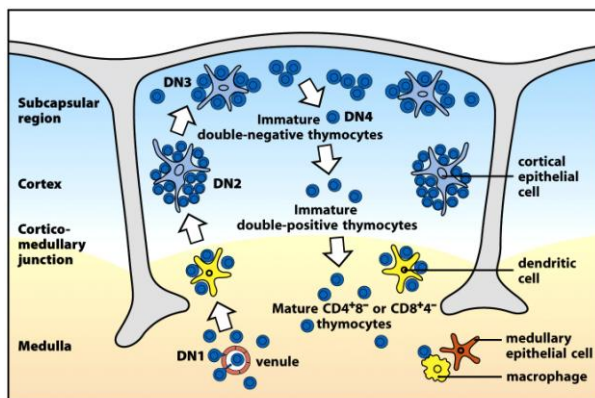


Figure 3

Thymocytes at different developmental stages are found in distinct parts of the thymus.

Earliest precursor thymocytes enter the thymus near the cortico-medullary junction.

Differentiation through DN stages (CD4- CD8-) until DP stage (CD4+ CD8+) takes place in the cortex. The medulla contains only mature

single-positive T cells, which eventually leave the thymus. (Janeway's Immunobiology, seventh edition)

It has been reported that upon maturation of T-cells (from DN- through DP- to SP-stage), expression of cell surface glycosyl-phosphatidylinositol–anchored protein CD24 (also known as heat stable antigen – HSA) decreases gradually (Kay et al., 1991). Conversely, the expression of the TCR/CD3-complex increases as T-cell maturation progresses (Bonifacino et al., 1990). Hence, the expression levels of these markers are often used as indicators of possible deregulations in T-cell development.

2.2. TCR-complex signaling

This section shall introduce TCR-mediated signaling in mature T cells, giving an overview of the main proteins involved and their interactions. This will be followed by a detailed description of the structure and function of the adaptor protein SRC homology 2 (SH2)-domain-containing leukocyte protein of 76 kDa (SLP76) and its role in a negative feedback loop regulating T cell activation.

Dendritic cells (DC) are specialized or professional antigen presenting cells (APCs). These cells link innate and adaptive immunity and have the ability to engulf, proteolytically process and present antigens on their cell surface. DCs express major histocompatibility complex (MHC) on their surface, which carry processed peptide antigens for efficient presentation to T-cells (Figure 4). As previously mentioned T-cells interact with APCs and scan their surface in search for non-self antigens. Activation occurs when a T-cell detects the presence of its specific antigen, loaded on the proper MHC, on the APC and triggers several intracellular signaling cascades.

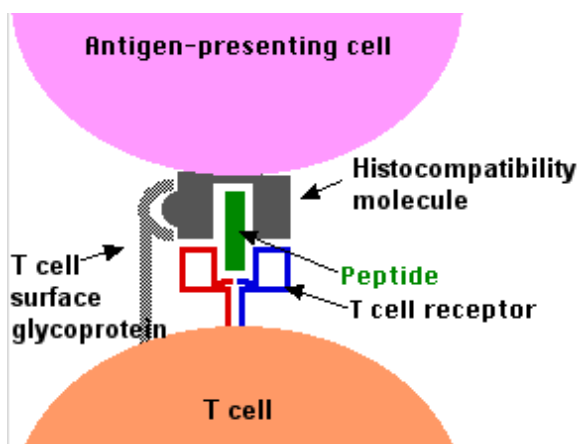


Figure 4

Antigen-presenting cell (APC) engagement with a T cell. The APC's histocompatibility molecule, loaded with an antigen peptide, binds to the T cell receptor and to co-receptor CD4 or CD8 (surface glycoproteins). These interactions trigger signaling events in the T cell.

A TCR-complex is composed of a heterodimer of variable subunits (either $\alpha:\beta$ or $\gamma:\delta$), responsible for antigen recognition and several invariant accessory chains (the CD3 ϵ , CD3 γ and CD3 δ and the ζ -chain/CD247) forming the signal-transducing module (Figure 5). Immediately after TCR stimulation, co-receptor bound lymphocyte-specific protein tyrosine kinase (LCK) phosphorylates Immunoreceptor Tyrosine-based Activation Motifs (ITAMs) in the intracellular domain of CD3 and ζ -chains. As a consequence, ζ -chain-associated protein kinase of 70 kDa (ZAP70) is recruited and activated to further phosphorylate the scaffold proteins SLP76 (Inoshima et al., 2012; Zhang et al., 1998) and Linker of activated T-cells (LAT) (Zhang et al., 1998). LAT is a transmembrane protein localized to cholesterol-rich membrane domains (lipid rafts). On the contrary, SLP76 is cytosolic in resting T-cells and constitutively bound to GRB2-related adaptor protein 2 (GRAP2, also known as GADS), an interaction dependent on the SH3-mediated binding of GADS to an Arg-Ser-Thr-Lys motif of SLP76. (*SH3-domains have a characteristic β -barrel structure, which normally binds to proline-rich amino acid sequences.*) Upon TCR stimulation, GADS binds with its SH2-domain to phosphorylated tyrosines of LAT, leading to translocation of the GADS-SLP76-complex to the membrane (Singer et al., 2004). (*SH2-domains bind to phosphorylated tyrosine motifs.*) Assembly of LAT-GADS-SLP76 provides a platform for the nucleation of a multimolecular complex that regulates initiation, amplification and duration of downstream signaling. Components of this include: the guanine-nucleotide exchange factor VAV1 and the adaptor non-catalytic region of tyrosine kinase (NCK), involved in actin cytoskeleton regulation; the interleukin-2-inducible T-cell kinase (ITK) and phospholipase C (PLC γ), controlling intracellular calcium and diacylglycerol levels; the adaptor Growth factor-receptor-bound protein 2 and the Son of Sevenless homologue (GRB2/SOS), activators of the Ras-ERK pathway; the integrin regulator Adhesion-and Degranulation-promoting Adaptor Protein (ADAP); the Hematopoietic Progenitor Kinase 1 (HPK1). Figure 6 presents an overview on the structure and functional domains on some of the signaling proteins mentioned above.

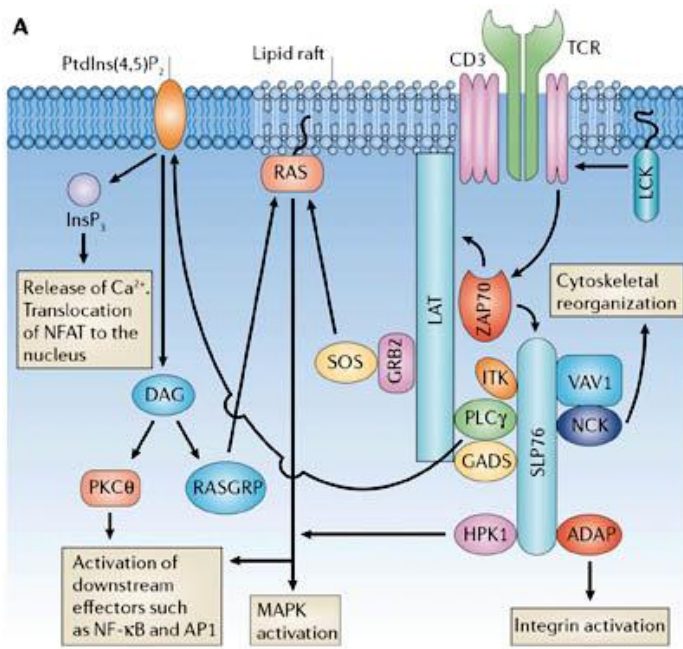


Figure 5

Role of SLP76 in signaling through the T cell receptor. Ligation of the T-cell receptor (TCR) by MHC complexed with antigen results in sequential activation of LCK and ZAP70. ZAP70 phosphorylates several downstream targets, including LAT and SLP76. SLP76 is recruited to membrane-bound LAT through its constitutive interaction with GADS. Together, SLP76 and LAT nucleate a multimolecular signaling

complex, which induces a host of downstream responses, including calcium flux, mitogen-activated protein kinase activation, integrin activation and cytoskeletal reorganization. (Koretzky et al., 2006)

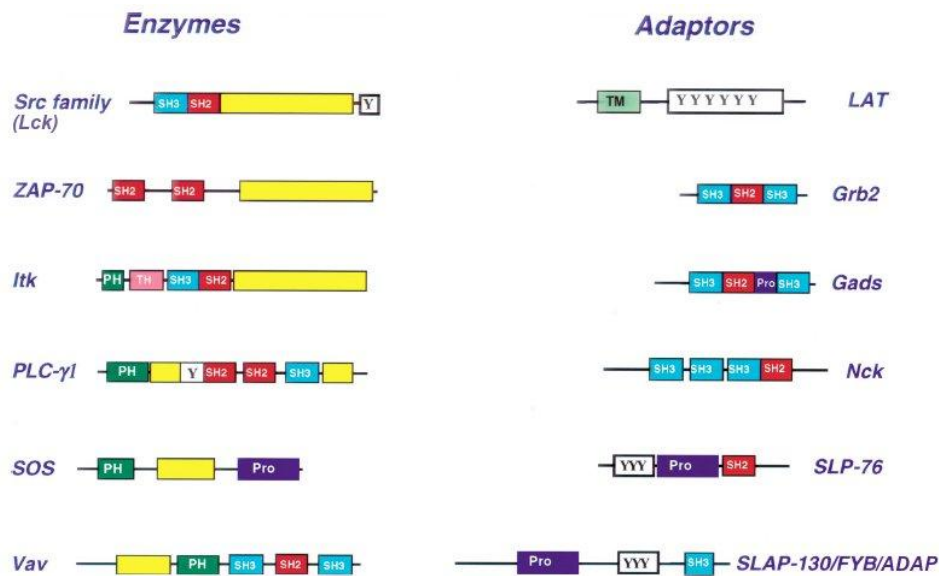


Figure 6

A selection of signaling proteins found in T lymphocytes depicted to highlight their modular structures. SH2, SH3 and PH domains are in red, blue and green respectively. A Tec homology domain is in pink, and a transmembrane domain is in light green. Sites of tyrosine phosphorylation are indicated with Y and proline-rich sites are indicated Pro. Domains with enzymatic function are in yellow (Samelson, 2002).

2.3. SLP76

SLP76 (Figure 7) has been intensively studied because of its critical role in both T-cell development and mature T-cell function. This scaffold protein is expressed throughout the hematopoietic compartment, e.g. in platelets, neutrophils, mast cells, macrophages, natural killer (NK) cells, T-cells and developing B-cells. Initial investigations in SLP76-deficient Jurkat cells (known as J14-cells) revealed that SLP76 is a positive regulator of TCR signaling (Motto et al., 1996). Phosphorylation of ZAP70, LAT and ITK were normal in these cells whereas PLC γ 1 phosphorylation and calcium flux were inhibited, indicating that SLP76 may link early signaling molecules to calcium release. Furthermore, up-regulation of CD69, a marker of T-cell activation, as well as of nuclear factor of activated T-cells (NFAT) and activator protein 1 (AP1) transcriptional activity were strikingly reduced (Yablonski et al., 1998). Analysis of SLP76 knockout mice revealed the complete absence of peripheral T-cells resulting from an early block in thymic development (DN3 to DN4 transition) (Clements et al., 1999).

SLP76 can be divided into an N-terminal domain, a central proline-rich domain and a C-terminal SH2 domain. The N-terminal domain comprises 3 tyrosines (Y112, Y128 and Y145), which upon phosphorylation can serve as binding-sites for VAV, NCK and ITK, respectively. Mutation of these three residues demonstrated their role in promoting calcium flux, PLC γ 1 phosphorylation and NFAT transcriptional activity (Fang et al., 1996; Yablonski et al., 2001). A fourth phosphorylatable tyrosine (Y173) has been recently identified, which is also required for TCR-induced phosphorylation of phospholipase C- γ 1 (Sela et al., 2011). Phosphorylation of all these sites is believed to be dependent on LCK- and/or ZAP70 protein kinases.

The regulatory p85 subunit of phosphatidylinositol 3-kinase (PI3K), ITK and LCK also bind to the proline-rich domain of SLP76. GADS and PLC γ 1 both bind to LAT and to the proline-rich domain of SLP76. Interestingly, mutation of the PLC γ 1 binding site on LAT not only abrogates binding to LAT, but also significantly decreases stability of SLP76-LAT-complex. These results highlight how multiple interactions within this molecular complex contribute cooperatively to the regulation of signal transduction.

Recruitment and activation of CDC42 through VAV1 and NCK bound to SLP76 activates both Wiskott-Aldrich syndrome protein (WASP) and p21-activated kinase 1

(PAK1), leading to actin polymerization (Bubeck-Wardenburg et al., 1998). On the other hand ITK has been reported to play a role in T-cell activation, cytokine secretion and development of $\alpha\beta$ T-cells as well as of non-conventional T-cells (August and Ragin, 2012).

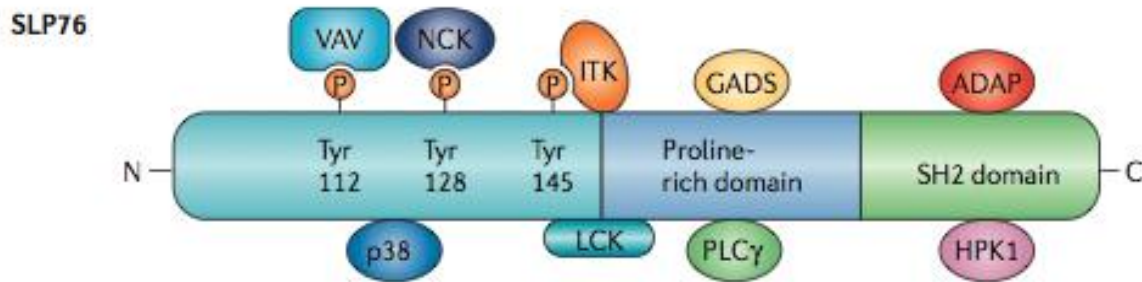


Figure 7

Structural features of SLP76. SLP76 contains inducibly phosphorylated tyrosines in the amino (N) terminus, a central proline-rich domain and a carboxy (C)-terminal SH2 domain. These domains mediate binding to several other signal-cascade intermediates as shown (Koretzky et al., 2006).

TCR engagement induces the SLP76- and ITK-dependent activation of PLC γ 1, that catalyzes the formation of second messengers inositol-1,4,5-triphosphate (InsP $_3$) and diacylglycerol (DAG) from phosphatidylinositol 4,5-bisphosphate (PIP $_2$). InsP $_3$ induces calcium release from the endoplasmic-reticulum, whereas DAG participates to the activation of protein kinase C (PKC) family members and Ras-MAP kinase pathway.

2.4. The C-terminal SH2 domain of SLP76 binds to ADAP and HPK1

ADAP is a positive regulator of LFA-1 integrin activation and signaling playing a key role in the formation of T-cell:APC conjugates (Wu et al., 2006). It has also been implicated in the regulation of T-cell survival, through the activation of NF κ B signaling pathway downstream of TCR and CD28 and the induction of the pro-survival factor Bcl-X $_L$ (Medeiros et al., 2007). T-cell proliferation and IL-2 production are impaired in ADAP deficient T-cells. However, ADAP effects on all the above-

mentioned functions are Ag-dose dependent, being more profound only at very low antigen-doses (Mueller et al., 2007).

Hematopoietic progenitor kinase 1 (HPK1), also known as MAP4K1, is a STE20-like protein serine/threonine kinase. In mammals, HPK1 is primarily expressed in hematopoietic cells and consists of an N-terminal kinase domain, a central proline-rich domain and a C-terminal citron homology domain (Figure 8). HPK1 activation and function depend on interaction with adapter proteins, as for instance with Grb2 family, Nck family, Crk family, SLP-76 family, and actin-binding adaptors like HPK1-interacting protein of 55 kDa (HIP-55). TCR-induced HPK1 phosphorylation at Y381 in humans (Y379 in mouse) mediates binding to the SH2 domain of SLP76 and therefore localization to the cell membrane. HPK1 has been implicated in a variety of signaling cascades and functions downstream of antigen-, growth factor- and cytokine-receptors, in apoptosis signaling and MAPK signaling.

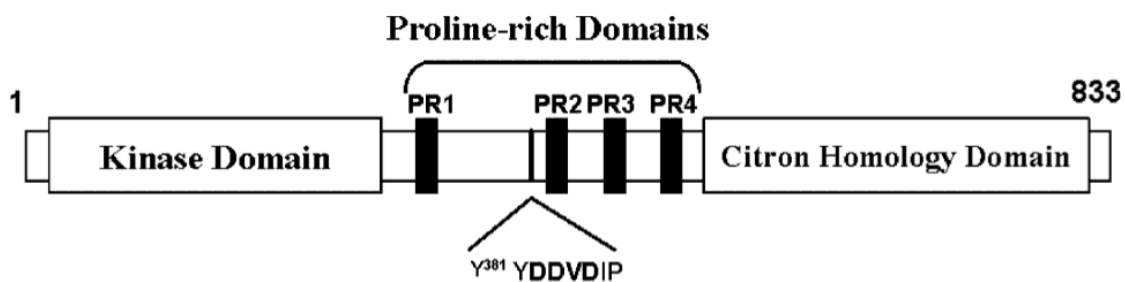


Figure 8

HPK1 structure. HPK1 contains an N-terminal serine/threonine kinase domain, a C-terminal citron homology domain, four proline-rich motifs (PR1, PR2, PR3, and PR4), a caspase cleavage site (DDVD). Phosphorylation of tyrosine residue 381 induces HPK1 binding to SLP-76 SH2 domain. (Boomer and Tan, 2005).

HPK1's ability to activate c-Jun N-terminal kinases (JNK) suggests a role in regulation of NFAT gene transcription and IL-2 production. JNK activation is shown to mediate T-cell proliferation, Th1/Th2 differentiation and activation-induced cell death (AICD) (Boomer and Tan, 2005).

Although HPK1 does not appear to interact directly with members of the MAPKs (Kiefer et al., 1996), overexpression of HPK1 in Jurkat cells has revealed a negative effect on Erk kinases and NFAT/AP1-dependent transcription (Liou et al., 2000; Sauer et al., 2001). Conversely, other groups showed that HPK1 enhances

both AP-1 and IL-2 transcription (Hu et al., 1996; Ling et al., 1999; Ma et al., 2001). HPK1 also has been implicated in NF- κ B activation, through IKK- α and - β activation, important for cell survival (Figure 9) (Hu et al., 1999). Studies in Jurkat cells have shown a constitutive binding of HIP-55 to HPK1. HIP-55-HPK1 complex negatively modulates NFAT-activity in cells stimulated by superantigen pulsed Raji B-cells. Interestingly, this effect can be reversed using kinase-dead HPK1 mutants, suggesting a kinase-dependent effect (Le Bras et al., 2004).

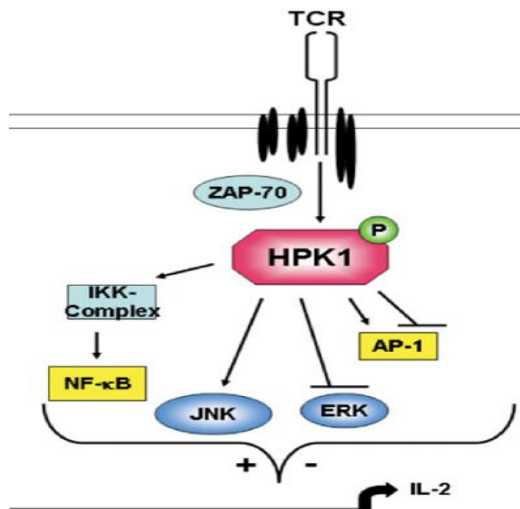


Figure 9

HPK1 function in TCR signaling. After TCR engagement, HPK1 is tyrosine phosphorylated and becomes activated. HPK1 may inhibit activation of ERK2, AP-1 and transcription of IL-2 gene. On the contrary, HPK1 may activate JNK, NF- κ B, AP-1, and IL-2 depending on the cell type and stimuli used. HPK1 is believed to play a pro-apoptotic role by activating JNK and inhibiting NF- κ B activation after caspase cleavage in T-cells. Arrows indicate activation while bars indicate inhibition. HPK1 is labeled in pink, transcription factors are colored in yellow, signaling molecules are shown in light blue and MAPK kinases are colored in dark blue. P = phosphate group (*green*) (Koretzky et al., 2006).

2.5. Immunological synapses and organization of signaling complexes

Antigen recognition during the interaction of a T-cell with an APC induces the formation of a specialized cell-cell interface called immunological synapse. This intercellular junction is formed by recruitment and spatial reorganization of multiple proteins at the site of interaction. In T-cells, the recruited proteins assemble in signaling complexes or signalosomes, also known as “microclusters” (MCs). In some instances, the latter may organize in higher-level structures named supramolecular activation clusters (Dustin et al., 2010). MCs consist of receptors, kinases, phosphatases, other enzymes and adaptor proteins that trigger various signaling cascades. Presumably, multiple protein-protein interactions within these signaling modules cooperatively contribute to their assembly and stability, consequently, regulating the kinetics of activation of downstream signaling pathways. In particular,

the SLP76-GADS-LAT complex constitutes a critical nucleation site for signaling MCs, hence, it is predicted to play a major role in influencing their stability. In conclusion, MCs are rather short lived, tightly regulated signaling modules, which are formed upon TCR stimulation. MC formation and dynamics have been studied in surrogate synapses formed between T-cells and anti-CD3 antibody-coated glass slides. This artificial interaction serves as a well-established model to dissect the underlying molecular mechanisms of MC formation in vitro. Molecules that are included into MCs can be either tagged by fluorescent proteins or detected by immunofluorescence, thereby allowing to visualizing MCs by confocal microscopy. We used the latter approach to determine the role of SLP76-14-3-3 interaction in MC-stability (Trautmann, 2005).

2.6. Physical and functional interaction between HPK1 and SLP76

In this section we will focus on the interaction between HPK1 and SLP76 and the role of these proteins in a recently discovered negative feedback loop regulating T-cell activation. Eventually, this will lead us to the introduction of our SLP76-S376A mouse mutant model, the presentation of our scientific questions and to an explanation of our methodical approaches in more detail.

As previously discussed, TCR-engagement triggers the activation of tyrosine kinases, LCK and ZAP70, by tyrosine-phosphorylations. Previous studies have shown that HPK1 can be phosphorylated by ZAP70 at Y379, and bind to the SH2 domain of SLP76 (Sauer et al., 2001), resulting in the recruitment of HPK1 to SLP76-containing microclusters (Lasserre et al., 2011). Moreover, it has been shown that knockout of HPK1 in mice (Shui et al., 2007) or its knockdown by RNA interference in Jurkat cells (Di Bartolo et al., 2007) results in increased TCR proximal activation, underscoring the negative regulatory function of HPK1. For instance, HPK1 knockout mice show increased activation of T-cells upon TCR stimulation, represented by more persistent calcium flux, phosphorylation of PLC γ 1 and Erk and increased cytokine production compared to wild-type mice (Shui et al., 2007). Interestingly, work conducted by the host laboratory has demonstrated that phosphorylation of residues S376 of SLP76 and T254 of GADS is controlled by HPK1 (Figure 10).

Moreover, these modifications are required for the association of 14-3-3 proteins (e.g. 14-3-3 ζ , ϵ and τ isoforms) to the SLP76-GADS complex (Di Bartolo et al., 2007; Lasserre et al., 2011). Mutation of these sites to alanine, abolishes their phosphorylation, therefore impairs 14-3-3 recruitment and increases stability of SLP76-containing microclusters as well as transcriptional activity of NFAT (Lasserre et al., 2011). Based on these data, a model has been proposed by which HPK1-induced recruitment of 14-3-3 proteins leads to disassembly of SLP76-GADS complexes from LAT-containing microclusters, consequently to a down-regulation of SLP76-mediated signaling and T cell activation (Lasserre et al., 2011).

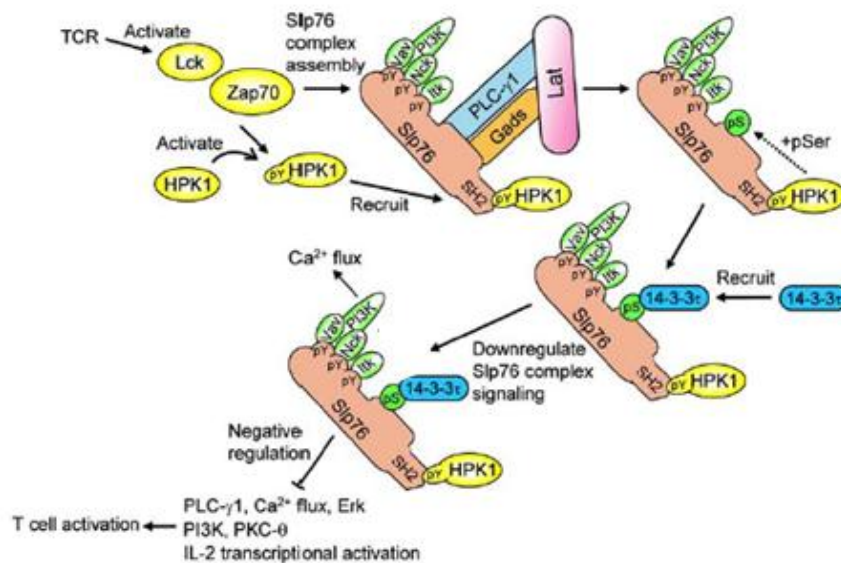


Figure 10
A schematic model of Slp76 regulation by HPK1 during T-cell signaling. Following TCR signaling, Lck is activated and phosphorylates Zap70, leading to phosphorylation and assembly of the Slp76

complex. Tyrosine phosphorylation of HPK1 by Zap70 results in HPK1 translocation to GEMs and binding to the SH2 domain of Slp76. HPK1 subsequently phosphorylates Slp76 (and GADS, not depicted) and induce recruitment of 14-3-3 proteins. The recruitment of 14-3-3 to the Slp76 complex may result in down-regulation of TCR signaling, including PLC- γ 1 and ERK phosphorylation as well as Ca²⁺ flux, leading to decreased IL2 transcription (Shui et al., 2007).

Several observations indicate that HPK1 may play a role in some pathological conditions. For instance, HPK1 knockout mice showed increased susceptibility to inducible experimental autoimmune encephalomyelitis (EAE), a murine model of multiple sclerosis (Shui et al., 2007). Moreover, a reduced expression of HPK1 has been proposed to contribute to autoimmunity in patients suffering from systemic lupus erythematosus (Zhang et al., 2011). HPK1 has also been implicated in the regulation of cytotoxic T-cells responses against cancer (Alzabin et al., 2010).

Indeed, HPK1 is activated in T-cells by the pro-inflammatory mediator prostaglandin E2 (PGE2), via a signaling pathway involving phosphorylation of HPK1 by the cAMP-dependent protein kinase (PKA) (Sawasdikosol et al., 2007). Importantly, HPK1-deficient T-cells were reported to be less sensitive to PGE2-mediated negative regulation of T-cell activation, showed increased levels of IL-2 production, increased cell proliferation as well as higher resistance to apoptosis compared to wild-type cells. Finally, HPK1 knockout mice were able to reject lung tumors that produce high amounts of PGE2 (Alzabin et al., 2010) although the molecular mechanism underlying this increased resistance to tumor development was not characterized. Interestingly, unpublished data obtained in the host laboratory have shown that treatment of T-cell lines with PGE2 does increase the interaction between 14-3-3 proteins with GADS and SLP76. This supports a potential regulation of the HPK1-dependent negative feedback loop, as described above, by PGE2.

2.8. Introduction of SLP76-S376A knock-in mouse

As previously mentioned, this S376 of SLP76 is phosphorylated by HPK1, providing a binding site for 14-3-3 proteins, which is crucial for the HPK1-mediated negative feedback loop on T-cell activation.

A possible scenario, based on previous data obtained by the hosting laboratory, predicts that mutation of this site would increase the strength and/or duration of TCR-induced signaling. This would be explained by a reduced or absent negative feedback regulation, similarly to what have been observed in HPK1 knockout mice. Such a modification in the signaling outcome may result in altered thymic selection and/or functional responses by mature T-cells. On the other hand, while HPK1 appears to also independently activate other signaling pathways (e.g. NFkB), mutation of the S376A is expected to specifically impair the HPK1-induced negative feedback loop acting on the SLP76- (and GADS-) dependent signaling axis (Figure 11A and 11B). Hence, the effects of SLP76-S376A mutation may only partially overlap with those of HPK1-deficiency.

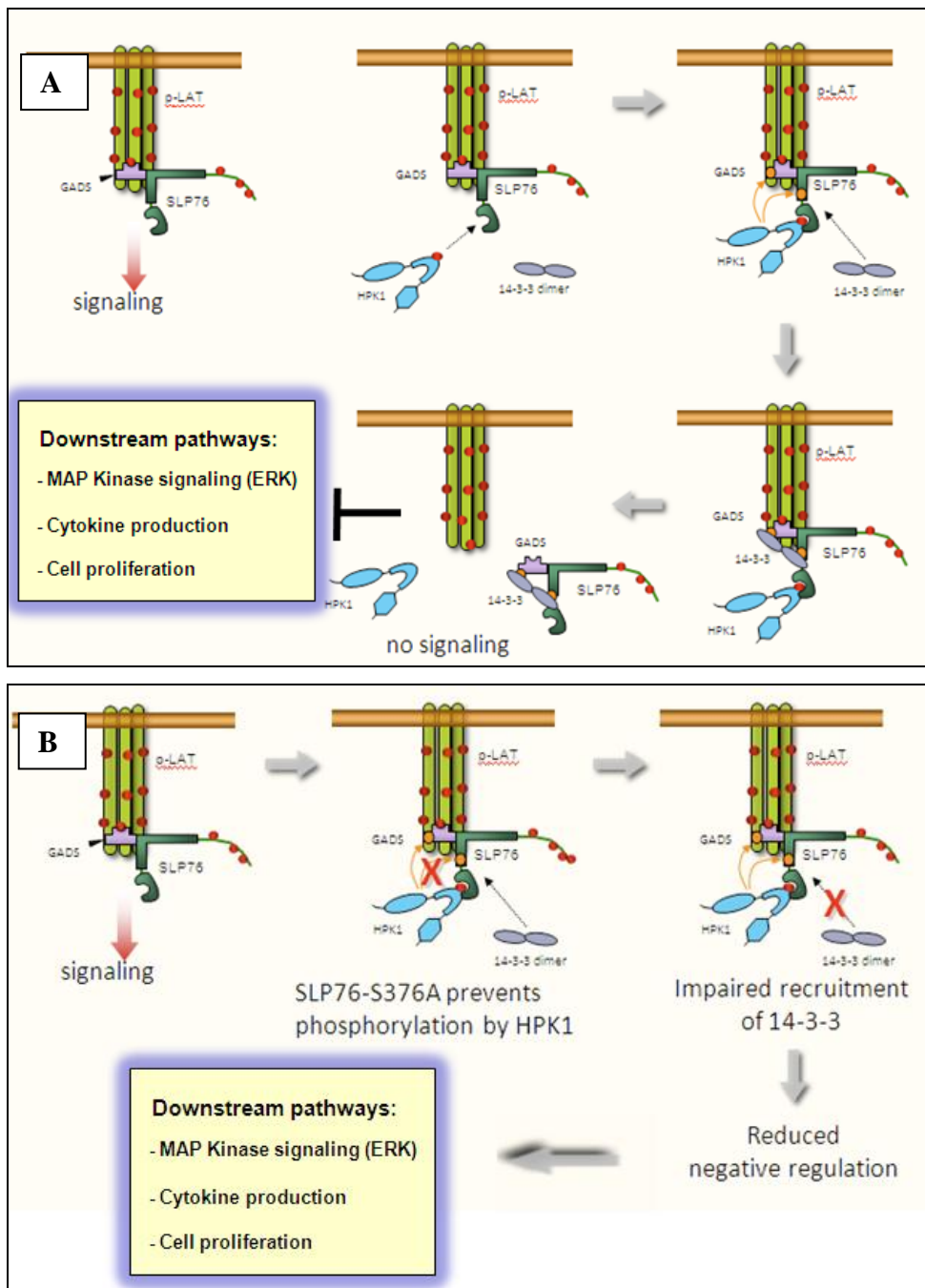


Figure 11

Model of regulation of stability of signaling microcluster and T-cell activation by HPK1. A) SLP76-GADS complex are recruited to the phosphorylated transmembrane adaptor LAT to form signaling-competent microclusters. When phosphorylated on Y381 (Y379 in mice), HPK1 is incorporated into microclusters by interacting with the SH2 domain of SLP76 and phosphorylates S376 of SLP76 and T262 of GADS. 14-3-3 proteins then bind to SLP76-GADS complexes through these phosphorylated residues, thus leading to dissociation of these complexes from phospho-LAT and terminating signaling. B) SLP76-S376A mutation prevents phosphorylation by HPK1, therefore impairing recruitment of 14-3-3 proteins and reducing negative regulation. (Lasserre et al., 2011)

To test these hypotheses, the host laboratory has recently generated a knock-in mutant mouse bearing a serine to alanine point mutation on the SLP76 protein at S376 (SLP76-S376A mouse). This model will allow studying the impact of this specific mutation on T-cells' development and function. Furthermore, it will enable us to address similar questions in other hematopoietic lineages expressing SLP76. This model will also be helpful to address the effect of the SLP76-S376A mutation in a pathological setting, such as cytotoxic T-cell responses against PGE2-producing solid tumors.

2.9. Aim of this work

The aim of this master's thesis was to contribute to the initial characterization of the SLP76-S376A mutant mouse model. In particular, my work focused on two points:

1. The analysis of T-cell activation and development in SLP76-S376A mice
2. The setup of an experimental cancer model to test the potential effects of the SLP76-S376A mutation on cytotoxic T cell responses *in vivo*.

For the developmental studies, I compared the proportions of different thymic subpopulations between wild type and mutant mice, by monitoring the expression of several markers including CD3, CD4, CD8, CD24, CD25 and CD44 in developing thymocytes.

In order to evaluate T-cell activation, I first used flow cytometry and western blot to analyze the phosphorylation of several proteins involved in T cell signaling pathways upon TCR stimulation. These included Erk kinases (pT202/pY204), SLP76 (Y128) and upstream regulators of the NFkB pathway such as PKC θ and IKK β .

In addition to that, I worked on a method to visualize and quantify microcluster-formation in mouse T-cells, using confocal microscopy. This approach was previously established in the host laboratory to demonstrate the effects of SLP76 and/or GADS mutations on the stability of SLP76- and LAT-containing signaling microclusters, in both Jurkat T-cells and primary human T lymphocytes (Lasserre et al., 2011).

I also analyzed the functional response of wild type and mutant T-cells *ex vivo* by measuring the production of cytokines and the proliferative response of T cells upon TCR and CD28 stimulation. Indeed, mutant T-cells were expected to be

hyper-responsive to TCR stimulation, hence, to proliferate more than wild type T-cells and/or produce more cytokines. In this respect, we chose to measure the production of IL-2, a well-known T-cell growth and differentiation factor produced by both CD4 and CD8 T-cells upon stimulation (Kish et al., 2005; Smith, 1988), and INF- γ , which is important for cell-mediated immune responses (e.g. anti-viral and anti-tumor immunity). Another reason for focusing on detection of INF- γ was because of its reference to CD8+ T-cell activation (Ikeda et al., 2002).

Finally, I started to generate new tools for the analysis of an anti-tumor response in SLP76-S376A and control mice. For this purpose, I used a Lewis lung carcinoma (LLC) cell line, which has previously shown to be efficiently rejected *in vivo* and killed *in vitro* by HPK1-deficient T-cells (Alzabin et al., 2010). My goal was to modify LLC cells by transfecting them with a reporter luciferase gene. This would allow us to easily visualize and quantify tumor growth and rejection by measuring luciferase-dependent bioluminescence in animals *in vivo* and/or *ex vivo*.

In conclusion, the experimental approaches outlined above led to the following results:

1. TCR-induced signaling was increased in SLP76-S376A compared to normal T-cells, as demonstrated by increased phosphorylation of ERK1/2 kinases.
2. Both CD4+ and CD8+ mutants T-cells exhibited increased proliferation and CD8+ mutant T-cells showed higher INF- γ production upon co-stimulation with agonist anti-CD3 and -CD28 antibodies.
3. No significant differences were observed in T-cell development between wild type and mutant mice.
4. Initial experiments demonstrated that a bioluminescent reporter LLC cell-line can be generated and that tumor formation can be measured both *in vivo* and *ex vivo* upon injection of these cells in mice.

3. Materials and Methods

3.1. Cell culture

3.1.1. B16-F10 mouse melanoma cell line

This cell line was obtained from Marc Daëron's lab laboratory (Institut Pasteur, Paris – France). B16-F10 cells were derived from B16 melanomas (malignant tumor of melanocytes) after selection for their ability to form metastases in the lung of C57BL/6J mice (Nicolson et al., 1978). B16-F10 cells grow *in vitro* as adherent cells with a mixed spindle shaped and epithelial-like morphology. They were cultured in Dulbecco's Modified Eagle's Medium (DMEM) supplemented with 10% FCS, 2mM Penicillin and 2mM Streptomycin and were split 3 times a week at a 1:6-ratio. In order to find a suitable cell line for a tumor rejection experiment this cell line was tested for Prostaglandin E₂ (PGE₂) expression, however, PGE₂ could not be detected in cell culture supernatant.

3.1.2. Lewis lung carcinoma

"Lewis lung carcinoma" (LLC or 3LL) was a gift of Dr. Karim Benihoud (Institut de Cancerologie Gustave Roussy, Villejuif - France). This cell line was derived from spontaneous lung tumors of the C57BL/6 mouse strain (Bertram and Janik, 1980) and was reported to be tumorigenic in C57BL/6 mice forming lung tumors. LLC cells express high levels of PGE₂, which was shown to be important for tumor engraftment in the lungs (Young and Knies, 1984). These cells were cultured in DMEM supplemented with 10% FCS, 2mM Penicillin and 2mM Streptomycin. The estimated doubling time for LLC cells is approximately 21 hours. LLC cells grow partly as monolayer and partly in suspension and were routinely split 3 times a week at a ratio of 1:5.

3.1.3. T8.1 cell line

T8.1 is a murine T-cell hybridoma expressing human CD4 receptor and a chimeric mouse ($C\alpha, C\beta$) – human ($V\alpha, V\beta$) – T-cell receptor (TCR) (Hogquist et al., 1994). It does not to express any detectable levels of PGE_2 , therefore, it served as a negative control for PGE_2 detection assays. The medium used for keeping T8.1 cells in culture was DMEM supplemented with 10% FCS, 2mM Penicillin and 2mM Streptomycin, 400nM methotrexate, 1mg/ml G418 and 50 μ M 2-mercapto-ethanol.

3.2. LLC transfection with pGL4.50 [luc2/CMV/Hygro] Vector

3.2.1. pGL4.50[luc2/CMV/Hygro] Vector

Lewis lung carcinoma cells have been transfected with a luciferase reporter vector (pGL4.50 [luc2/CMV/Hygro] vector) (Figure 12). The goal was to set up a technique for “*in vivo* tumor detection”, using a bioluminescent luciferase reporter cell line. The plasmid used is 6600bp of size and carries a CMV (cytomegalovirus) immediate early enhancer/promoter for high translational expression. It contains a hygromycin B -resistance gene for mammalian cell selection as well as an ampicillin resistance gene for bacterial selection (vector amplification). Furthermore, this vector encodes the luciferase gene “luc2” derived from the common eastern firefly (*Photinus pyralis*). A SV40 late poly (A) signal sequence is positioned downstream of luc2 for efficient transcription termination. This vector was obtained from “Promega” - Catalog#E1310.

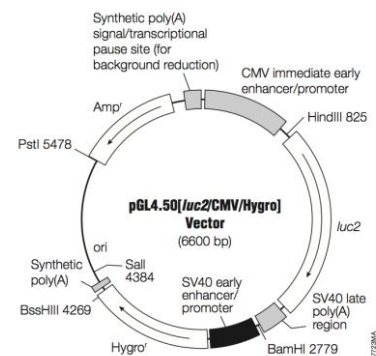


Figure 12

pGL4.50[luc2/CMV/Hygro] Vector

3.2.2. Transfection of LLC cells using FuGENE® 6 Transfection Reagent

One day before transfection, LLC cells were seeded in a six well plate at 3 different cell concentrations: 0.5×10^6 , 1×10^6 or 2×10^6 per well. The day of the experiment the culture medium was replaced with serum free medium (SFM - DMEM); the plasmid DNA complex was mixed with the FuGENE 6 transfection reagent (Roche Applied Science). 97 μ l of SFM were dispensed into a 1.5 ml Eppendorf tube. Then 3 μ l of FuGENE 6 reagent were added directly into the medium followed by addition of 1 μ g of the pGL4.50 [luc2/CMV/Hygro] vector. For efficient stabilisation of the FuGENE – plasmid DNA complex, reagents were incubated for 15 minutes at room temperature. After incubation, 100 μ l of FuGENE – plasmid DNA complex were added to LLC cells (at 60% - 80% confluency) in a 6-well plate, by pipetting the solution in a dropwise manner across the well.

After further 6 hours incubation at 37°C, culture medium was exchanged with complete medium supplemented with FCS. Three days later transfected cells were selected by adding hygromycin to the culture medium at two concentrations: 0.8mg/ml and 1mg/ml. Cells selected with 0.8mg/ml are referred to as *LLC – LUC2/0.8*, whereas those selected with 1mg/ml are referred to as *LLC – LUC2/1*. Significant growth of *LLC – LUC2/0.8* cells was observed after 3 weeks of selection in hygromycin-containing medium, whereas recovery of *LLC – LUC2/1* required 4 weeks. During the selection period dead cells were occasionally removed, but cells were never split.

3.3. Prostaglandin E₂ (PGE₂) detection

For detection of PGE₂ the DetectX® “Prostaglandin E₂ high sensitivity immunoassay kit” (Arbor Assays LLC, Michigan, USA) has been used. The following cell lines were examined for PGE₂ production: Lewis lung carcinoma (LLC), *LLC – LUC2/1*, *LLC – LUC2/0.8*, B16-F10 mouse melanoma, T-cell hybridoma T8.1 (used as negative control).

3.3.1 Procedure and assay principle

This kit allows the detection of PGE₂ present in the samples by competitive immunoassay. Cells were counted and equally distributed into a 96-well plate in complete culture medium. After two days, 200µl of supernatant was taken as sample for each cell line. Samples were diluted in a 1:5 and 1:10 ratio before starting the assay. 100µl of samples were distributed into a 96 well plate coated with goat anti-mouse IgG, provided with the kit. Thereafter, the following reagents have been added to each well: 100µl of assay buffer, 25µl “DetectX® Prostaglandin E₂ Conjugate” (PGE₂ conjugated to horseradish peroxidase: PGE₂-HRP), 25µl “DetectX® Prostaglandin E₂ high sensitivity antibody”. The binding reaction was initiated by adding the mouse monoclonal high sensitivity antibody against PGE₂. Hence, PGE₂ contained in samples or PGE₂-HRP could bind to the anti-PGE₂ antibody and were captured by anti-mouse IgG antibody, previously immobilized to the bottom of the wells. After 16 hours incubation at 4°C, each well is washed 4 times with 300µl washing buffer, then dried and 100µl of TMB substrate were added to each well. After 30 minutes incubation at room temperature, the peroxidase reaction was stopped and measured by reading the optical density at 450nm. PGE₂ concentrations of samples were determined using a standard curve prepared with the provided PGE₂ standard.

3.4. Mice

C57BL/6 mice were purchased from Elevage Janvier (Le Genest Saint Isle, France). The SLP76-S376A knock-in mice were generated by the “Plate forme d’Exploration Fonctionnelle du Système Immunitaire de la Souris” (Marseille, France). These mice were generated on a mixed 129 x C57BL/6 background, then backcrossed on C57BL/6 background for more than 8 generations. All animals were healthy reproduced with Mendelian ratios and had a normal life span. Concerning lymph node and spleen tissue of the mutant, there were no remarkable changes in cell numbers and no further anomalies noticed.

3.5. CD4+ or CD8+ T-cell purification

Untouched CD4+ or CD8+ T-cells from mice were isolated by negative selection (or depletion), using commercially available CD4+ (or CD8+) T-cell isolation kits respectively (Miltenyi Biotec). Spleen and lymph nodes from mice were dissociated and cells pooled to maximize T-cell recovery. Cells were resuspended in MACS-buffer (PBS, 0,5%BSA, 2mM EDTA - 40µl per 10⁷ total cells) before incubation for 20 minutes at 4°C with a “biotin-antibody cocktail” (10µl per 10⁷ total cells). This biotin-antibody cocktail contains antibodies directed against the following surface markers: CD8 (or CD4), CD11b, CD11c, CD19, CD45R, CD49b, CD105, MHC class II and Ter119.

These antibodies allowed to mark and remove all unwanted cell types from the sample, e.g.: CD8+ (or CD4+) T-cells, B-cells, dendritic cells, NK-cells, macrophages, granulocytes, endothelial cells and erythroid cells.

After incubation with biotin-antibody cocktail, cells were washed by adding MACS-buffer (30µl per 10⁷) before incubating 20 minutes at 4°C with “anti-biotin micro beads” (20µl per 10⁷). These magnetic micro beads, conjugated to monoclonal anti-biotin antibodies, allowed capturing all the cell types previously labeled with biotin-conjugated antibodies. Samples were applied to a magnetic column of an autoMACS Pro Separator and sorted using the “DepleteS” (S = sensitive) program. Unlabeled CD4+ (or CD8+) T-cells were collected in the flow-through (first fraction). On the other hand, all cell types bound to the micro-beads were retained by the magnetic column during the separation procedure and collected in the second fraction.

3.6. Activation-induced phosphorylation experiments, using western blot

3.6.1. T-cell activation using soluble biotin labeled anti mouse CD3ε and CD28 antibodies

Different techniques were employed for *in vitro* activation of T-cells. Activation using cross linking of biotin-labeled anti-mouse CD3ε and biotin CD28 antibodies was used for detecting changes in phosphorylation of intracellular signaling proteins.

We chose fluorescence activated cell sorting (FACS) and western blot as read out for these experiments.

Once CD4⁺ (or CD8⁺) T-cells were purified and counted, they were resuspended in OPTI-MEM – medium and kept on ice. Cell-concentration varied between 15x10⁶/ml and 30x10⁶/ml. 100µl were taken out (corresponding to approximately 1.5 to 3x10⁶ cells) before activation and kept on ice until the end of the experiment (non-activated negative control). Opti-MEM antibody mix (Opti-MEMAb-mix) was prepared at a concentration of 10µg/ml for biotin labeled anti-mouse CD3ε and anti-mouse CD28 antibodies.

3.6.2. Activation for western blot

Streptavidin molecules, which display a very high affinity for biotin, were used to cross-link biotinylated molecules (e.g.: anti-CD3 and anti-CD28), thereby clustering receptors at the cell surface and triggering signal transduction. This approach serves as a well-established method to induce activation-dependent T-cell signaling cascades. Briefly, cells were centrifuged at 930xg for 8 minutes at 4°C and resuspended in Opti-MEMAb-mix. Following 30 minutes of incubation on ice, cells were washed twice in Opti-MEM at +4°C. A water bath as well as an Opti-MEM streptavidin solution (Opti-MEM-StrAv) at 5µg/ml final concentration, were equilibrated at +37°C. To start the activation, cells were kept in one single tube and Opti-MEM-StrAv was added after centrifuging and aspirating the supernatant. Immediately after resuspension in Opti-MEM-StrAv cells were put into the 37°C water bath. For each time point, a 100µl aliquot was taken out and transferred into previously prepared Eppendorf tubes containing ice-cold “stopping buffer”. Stopping buffer contains phosphatase inhibitors to prevent removal of activation induced phosphorylation. Immediate centrifugation for 8 minutes at +4°C was followed by addition of 30µl of cell-lysis buffer to the cell pellet. After 10 minutes incubation on ice, tubes were centrifuged at 13000g for further 10 minutes before transferring supernatant into new Eppendorf tubes. This step served for the elimination of detergent-insoluble material, including nuclei and free DNA, which might interfere with western blotting. At this point, proteins were stored overnight at -80°C.

3.6.3. Protein quantification

After cell lysis protein concentration in each sample was quantified in order to load equal protein amounts in each gel lane. *DC™ Protein Assay* kit (Bio-rad) was used for this purpose, according to the manufacturer instructions. Quantification was performed in a 96-well plate using a BSA standard curve. As mentioned in the handbook, 20 μ l of reagent S was added to 1ml of reagent A, therefore creating reagent A'. 5 μ l of BSA standard or 4 μ l of total protein samples were added to a 96-well plate, followed by addition of 25 μ l of reagent A' and thereafter 200 μ l of reagent B (to each well). After incubating samples with reagent mix for 15 minutes at room temperature, optical density at 690nm was determined. Protein concentration was calculated from sample's optical density by comparison with the BSA standard curve. Usually 4 μ g of total protein were loaded in each gel lane.

3.6.4. Polyacrylamide gel electrophoresis

An appropriate volume of protein lysates was diluted to 22.75 μ l and mixed with 8.75 μ l 4x NuPAGE LDS sample buffer and 3.5 μ l reducing agent, then heated at +70°C for 10 minutes for protein denaturation. Samples were then cooled at room temperature and loaded on Criterion™ XT precast gels (4-12% Bis-Tris, 18-well comb, 1.0mm thickness). 10 μ l of protein ladder (consisting of 4.5 μ l Precision plus protein™ all blue standards (Bio-Rad), 7.5 μ l 4x NuPAGE LDS sample buffer and 18 μ l distilled H₂O) was used to estimate the relative protein mobility. Finally, the gel was placed in the appropriate tank with 500ml MOPS running buffer and proteins were fractionated by applying an electric field (170 Volt) for approximately one hour

3.6.5. Protein transfer to membrane (blotting)

Following electrophoresis, proteins were transferred from the gel to a nitrocellulose membrane (LI-COR Bioscience, USA). The set up for this transfer was done as shown below in Figure 13.

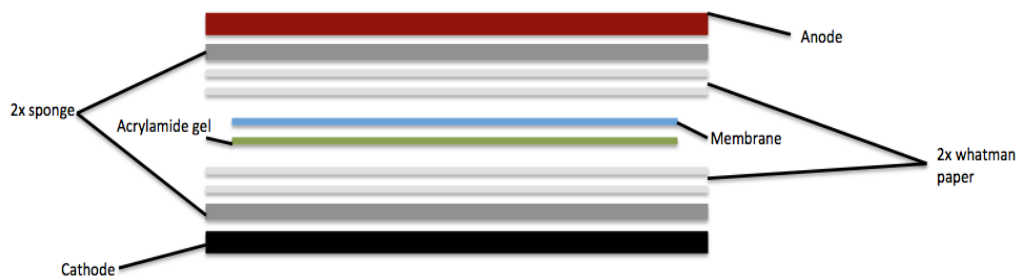


Figure 13

Protein blotting

apparatus. From top to bottom: Anode (red), sponges (grey), Whatman 3MM

paper (light grey), membrane (light blue), polyacrylamide gel (green), Cathode (black). When current is applied proteins migrate to the anode, therefore transfer from acrylamide gel to membrane occurs.

Transfer buffer (25mM Tris, 192mM glycine, 20% ethanol), an ice-cold cooling pack and a stirring magnet were added to the Criterion transfer tank containing the transfer assembly as shown above, before applying an electric field (100V) for 90 minutes.

After protein transfer, membrane was treated with Ponceau S (1:64-dilution) for approximately 5 minutes for total protein staining. A picture of the membrane was taken using a common copy machine. Subsequently, membrane was destained by incubation in Tris-buffered saline (TBS).

Membrane was treated with Blocking Buffer for Fluorescent Western Blotting (Rockland) for one hour at room temperature. This step is necessary to prevent unspecific antibody binding to the membrane. Blocking buffer was then removed and primary antibody solution (1:1 mix of TBS-0.1% Tween20 (TBST) and blocking buffer, containing the appropriate antibody) was added for 2 hours at room temperature or over night at +4°C. After washing the membrane three times with TBST for 5 minutes, the appropriate secondary antibody (coupled to either AF680 or DyLight800 fluorochromes) was diluted in 1:1 TBST-blocking buffer and added for 30 minutes at room temperature. After washing the membrane as explained above, the membrane was stored in TBS until fluorescence detection and quantification using an Odyssey near-infrared scanner (LI-COR Biosciences USA). The phosphorylation of following proteins was monitored: Lat (Y191), Erk1/2 (pT202+pY204), SLP76 (Y128), PLCγ1 (Y783), IKK-α/β (S181/180), PKCθ (T538).

3.7. Flow cytometry experiments

Flow cytometry (FCM) experiments were performed using either a BD FACSCalibur flow cytometer or Miltenyi biotech MACSQuantAnalyzer. FCM is a robust technique widely applied in immunology research. Among other applications, it allows to identify (and sort) different cell populations with distinct features or markers. These “markers” are usually recognized by specific antibodies, which are labeled with distinct fluorochromes, thus allowing the identification of each population in the flow cytometer.

As described in the introduction stimulation of T-cells triggers a plethora of intracellular signaling pathways. We were interested in early T-cell receptor (TCR) signaling initiated by LCK (lymphocyte-specific protein tyrosine kinase) mediated phosphorylation of ITAM's (immunoreceptor tyrosine-based activation motif) in the CD3-chains and eventually down to SLP76 (SH2 domain containing leukocyte protein of 76kDa), LAT (Linker of Activated T cells), PLC γ 1 (Phospholipase C γ 1) and Erk (extracellular-signal-regulated kinase or classical MAP kinase) phosphorylation. Moreover, we were interested in downstream activation events, such as cytokine production and cell-proliferation. Finally, we also investigated changes in thymic T-cell development using specific markers to follow the maturation-dependent generation of the major thymocyte subsets.

All FCM data analyses were performed using Flow Jo (Tree Star Inc, USA) software.

3.7.1. Activation-induced phosphorylation experiments, using flow cytometry

3.7.1.1. T-cell activation for phosphorylation experiments using FCM

For each kinetics time point, cells were activated in a separate eppendorf tube containing 100 μ l of cell suspension (corresponding to approximately 1.5 to 3 \times 10⁶ cells/tube) Incubation with Opti-MEMAb-mix and activation with Opti-MEM-StrAv were done as mentioned above always using 100 μ l per tube. Activation was stopped by immediate fixation of cells by adding 100 μ l of 8%PFA (leading to a final

concentration of 4% PFA). After incubating 10 minutes at room temperature, cells were washed twice with 500 μ l PBS to remove PFA and resuspended in FCM buffer.

3.7.1.2. Detection of phosphorylation

After stopping cell activation by PFA fixation, 2 washes in 500 μ l PBS were necessary to remove PFA. Following the first wash, cells were transferred to 5ml tubes. After the second wash PBS was aspirated and 500 μ l ice-cold methanol was added drop by drop while vortexing. Methanol treatment allows permeabilization of cells and was performed for 10 minutes at +4°C. Cells were then immediately subjected to the staining procedure or stored at -20°C and treated later on. Following methanol incubation, cells were centrifuged at 2000rpm for 8 minutes, then methanol was aspirated and cells resuspended in FCM buffer (PBS, 2.5%FCS, 0.02% sodium azide). Subsequently, staining of surface and intracellular proteins were performed at the same time (CD4-FITC, CD8-APC, rabbit anti-pErk/anti-rabbit-AF647, pSlp76-AF647). Cells were transferred into a 96-well plate, resuspended in previously prepared antibody mix and incubated for 45 minutes at +4°C. After incubation two washes with FCM buffer were performed, to eliminate antibody excess before resuspending cells in 200 μ l FCM buffer. Samples were immediately analysed by using a MACSQuantAnalyzer (Miltenyi Biotec).

3.7.2. Cytokine production assay

3.7.2.1. Pre-coating 96-well plates for cytokine production assay

50 μ l of an anti-mouse CD3 ϵ solution (10 μ g/ml in PBS) were distributed into a 96-well plate. For negative controls 50 μ l PBS was added into the wells. The plate was then sealed and incubated over-night at +4°C. The following day, antibodies had adhered to the plate's surface; unbound antibodies were removed by washing once with PBS.

3.7.2.2. Detection of cytokine production

For this assay, we used 96-well plates pre-coated with stimulatory antibodies as mentioned above. Before starting the experiment 75 μ l of a 20 μ g/ml “anti mouse CD28 antibody solution” (in complete culture medium) or 75 μ l of “Phorbol 12-myristate 13-acetate (PMA) – plus calcium ionophore (A23187) solution” was added to sample- or control-wells respectively. Incubation with complete culture medium for 45 minutes at 37°C was necessary to block unspecific binding sites on plastic wells. The PMA – calcium ionophore mixture triggers strong T-cell activation, hence cytokine production, and is therefore typically used as a positive control. Total LN cells were resuspended in complete culture medium at a cell concentration of 6.6x10⁶/ml. By adding 75 μ l of LN cells, the final concentration of anti mouse CD28 antibody was reduced to 10 μ g/ml. Final concentrations of and calcium ionophore were 50ng/ml and 0,5 μ g/ml respectively.

After 2 hours of incubation at 37°C, brefeldin A (BFA) was added to each well to a final concentration of 1 μ g/ml. BFA is reported to induce retrograde protein transport from the Golgi apparatus to the endoplasmic reticulum (ER). Thus leading to the accumulation of cytokines in intracellular compartments and preventing their secretion. This facilitates detection of cytokine expression by FCM. Further incubation for 4 hours at 37°C, was necessary to accumulate detectable amounts of the cytokines of interest.

Cells were then removed from the plate by pipetting thoroughly up and down and washed twice in FCM buffer (PBS, 2.5%FCS, 0.02% sodium azide), spinning down 5 minutes at 1500rpm. Cells were resuspended and incubated 30 minutes at +4°C in the antibody solution. CD4-FITC and CD8-APC conjugated antibodies were used for the surface staining of T-cell subsets. Subsequently, cells were washed twice in FCM buffer then incubated in 100 μ l fixation/permeabilization buffer (BD Biosciences) for 20 minutes at +4°C. This incubation was followed by two washes with Perm/Wash buffer (BD Biosciences). From this moment onwards, washes were performed with Perm/Wash buffer, diluted 1:10 with distilled water. IFN- γ -PE and IL-2-PE antibodies diluted Perm/Wash buffer were used for intracellular staining. Cells were incubated in antibody solution for 15 minutes, at room temperature. After

incubation, cells were washed twice in Perm/Wash buffer and finally resuspended in FCM buffer. All the washing steps included centrifugation for 5 minutes at 930xg. Experiment was immediately read on a MACSQuantAnalyzer (Miltenyi biotech).

3.7.3. Proliferation assay

3.7.3.1. Pre-coating 96-well plates for proliferation assay

Pre-coating of 96-well plates with stimulatory antibodies for proliferation assay was performed in a similar way as mentioned above for the cytokine production assay, with slight modifications. Antibody mix solution contained anti-mouse CD3 ϵ and CD28 antibodies in PBS, at a concentration of 5 μ g/ml and 10 μ g/ml, respectively. The procedure was continued as mentioned above. Hence, both anti-mouse CD3 ϵ and anti-mouse CD28 antibodies were adsorbed on to the plate's surface, whereas for the cytokine production assay the anti-CD28 antibody was added in a subsequent step in solution. Adding soluble anti mouse CD28 resulted in improved detection of cytokine production.

3.7.3.2. Mouse T-cell proliferation assay

This assay is based on the loss of a dye named carboxyfluorescein succinimidyl ester (CFSE) by stained cells, during their proliferation. CFSE is a viable fluorescent dye with an emission maximum at 517nm (detectable in the FITC channel) that covalently bind to cellular proteins. At each cell division, cells lose CFSE signal because of the dilution of labeled proteins between daughter cells. Hence, measuring dye dilution by analyzing cells with a flow cytometer, allows counting of the number of divisions performed by each cell in the population.

The assay was performed by stimulating cells in 96-well plates, which were pre-coated with antibodies as mentioned above. Before starting the assay, 100 μ l complete culture medium was distributed into relevant wells and incubated for 45 minutes to block unspecific binding of cells to the plastic surface of wells. Meanwhile

a 10 μ M CFSE solution in PBS was prepared for staining lymph node cells. Lymph nodes cells were dissociated counted and resuspended in Opti-MEM medium at a cell concentration of 5x10⁶. CFSE solution was mixed with cells in a 1:1 volume ratio and incubated for 15 minutes at +37°C. Subsequently, two washing steps were performed with 5ml complete culture medium. Afterwards, cells were distributed into the pre-coated and blocked 96-well plate (100 μ l per well corresponding to 500.000 cells) and incubated at 37°C.

After 72 hours, the plate was centrifuged at 1500rpm for 8 minutes and supernatant was removed. 50 μ l PBS were added to each well and thoroughly pipetted up and down to detach cells. Subsequently, cells were washed once in 100 μ l PBS, resuspended in 50 μ l antibody mix containing CD4-PE and CD8-APC in PBS, then incubated for 45 minutes at +4°C. Finally, cells were washed twice, resuspended in 200 μ l FCM buffer and immediately analyzed using a MACSQuantAnalyzer (Miltenyi biotech).

3.7.4. Thymic T-cell development

T-cell development in the thymus is essential for central tolerance. Aberrant regulations during this process can create an imbalance, leading to enhanced autoimmune reactions. We analyzed potential alteration in thymocyte development in SLP76-S376A knock-in mice by assessing the expression of common maturation markers, including the co-receptors CD4 and CD8, the TCR-associated CD3 ϵ chain and other membrane proteins such as CD24 (or HSA – heat stable antigen), CD25 and CD44.

Thymi were dissected and dissociated as described for spleen and lymph nodes. Cells were counted and resuspended in complete DMEM culture medium at a cell concentration of 15 x10⁶/ml and 200 μ l/well were distributed on a 96-wellplate (corresponding to 3 x10⁶ cells) for antibody surface staining. Cells were centrifuged for 8 minutes at 930xg, washed twice with FCM buffer before adding the antibody mix. Cells were then incubated 45 minutes at +4°C, washed twice in FCM buffer and finally resuspended in 200 μ l FCM buffer. Experiment was immediately read using a MACSQuant Analyzer (Miltenyi biotech).

3.8. Immunofluorescence and confocal microscopy

3.8.1. T-cell activation using anti-mouse CD3 ϵ and CD28 antibody-coated coverslips for immunofluorescence

The aim of these experiments was to visualize the activation-dependent assembly of signaling protein complexes (microcluster) in T-cells, using confocal microscopy. In order to achieve efficient coating with the stimulating antibodies, glass coverslips were first incubated with poly-L-lysine, which provides binding sites for the activating antibodies. Subsequently, coverslips were incubated with anti-mouse CD3 and CD28 antibodies. Cells were activated by dropping them on the cover slips and activation was stopped by fixation using 4% PFA. After washing carefully with PBS cells were permeabilized with saponin, stained with anti phospho-Lat (Y191) and anti-phospho-SLP76 (Y128) antibodies.

3.8.1.1. Preparation of antibody coated coverslips

Coverslips were cleaned by soaking them in 50ml of a 70% ethanol, 1N HCl-solution. After incubation for 10 minutes, two washes with distilled water and one wash with 70% ethanol were performed. Subsequently, coverslips were dried before distributing them into a 24-well plate (one coverslip per well). 2ml of a 1/10 poly-lysine dilution was added to each well, followed by 30 minutes incubation at room temperature. Coverslips were again completely dried on Whatmann paper. Incubations with the ethanol-HCl solution as well as with poly-L-lysine were performed on a shaker.

3.8.1.2. Coating with anti mouse CD3 ϵ and anti mouse CD28 antibodies

Poly-L-lysine-coated coverslips were treated further with anti-mouse CD3 ϵ and CD28 antibodies in the following manner. Two square pieces of Whatmann 3MM paper (big enough to fit the desired number of coverslips) were made wet with water and put on a flat surface (e.g.: small plastic tray). An equally sized piece of parafilm strip was placed on top of wet paper sheets.

The parafilm serves as a surface for applying 80 μ l drops of antibody mix solution (antibody mix solution: 10 μ g/ml for hamster anti mouse CD3 ϵ [clone 145-2C11] and 10 μ g/ml for hamster anti-mouse CD28 [clone 37.51]). One poly-L-lysine coated coverslip was placed on top of each drop. Plastic tray was sealed and incubated over night at +4°C. The wet Whatmann 3MM paper provides sufficient humidity during the incubation, since it is crucial not to let completely dry antibody-coated coverslips.

3.8.2. T-cell activation on coverslips pre-coated with anti-mouse CD3 ϵ and anti-mouse CD28

After over night incubation at +4°C, coverslips were pre-coated with activating antibodies. A 24-well plate was filled with PBS (1ml per well) before transferring each coverslip into one well, antibody coated side facing up. PBS was aspirated and coverslips were washed again with 1ml pre-warmed PBS, to get rid of antibody excess. Subsequently, PBS was removed and 200 μ l of RPMI medium containing 10%FCS was added to each well. The 24-well plate was incubated at +37°C for 45 minutes. This was performed to block unspecific antibody binding sites on the coverslips.

For activation on coverslips we used purified CD4+ or CD8+ T-cells. After purification, cells were resuspended in serum-free RPMI medium at a cell concentration of 5x10⁶/ml. An aliquot was kept as negative control, whereas the rest of the sample was resuspended in RPMI supplemented with 10%FCS. We used coverslips, pre-coated with poly-L-lysine as a negative control, since, in the absence of stimulating antibodies cells were not activated and microcluster formation was hardly detectable. For these negative control samples, no serum is added to medium in order to favour the attachment of cells to coverslips. Activation was performed by putting the 24-well plate containing coverslips into a 37°C water bath and dropping 200 μ l of either sample or negative control cells (appr. 1x10⁶ cells) on the centre of each slide. Negative controls have been incubated at +37°C for 5 minutes, before being fixed by adding 200 μ l 8%PFA and incubating at room temperature for 10 minutes. Finally, PFA was removed by two washes in PBS. Samples were activated in the same way, however, a kinetics was performed by incubating cells on anti-CD3 and –CD28 coated coverslips for 3,5 and 7 minutes before fixing them with PFA.

3.8.3. Immunofluorescence staining

Following two washes in PBS, coverslips were incubated for 10 minutes in 50mM NH₄Cl, followed by two additional washes in PBS. NH₄Cl treatment is required to quench unreacted aldehydes and prevent covalent binding of staining antibodies to proteins. Subsequently, cells were permeabilized before proceeding with intracellular staining against phosphorylated SLP76 (Y128) and LAT (Y191). Cells were incubated for 15 minutes in permeabilization buffer containing 2% BSA, 0.05% Saponine in PBS. This buffer was used throughout all subsequent washing and antibody staining. Antibody mixture for pSLP76 and pLAT was prepared. 80µl drops were distributed on a flat surface as mentioned in paragraph **3.8.1.2.** and coverslips were applied onto antibody drops with the cell-attached side facing down. After incubation with primary antibody for 45 minutes at room temperature, coverslips were washed three times then incubated for 45 minutes with secondary antibodies. Finally, three additional washes in permeabilization buffer were performed. To avoid fast bleaching of the fluorochrome-signal, a Mowiol-Dabco mixture was used as medium to mount coverslips on microscope glass-slides. Slides were left in the dark at room temperature over night, before performing analysis by confocal microscopy. (Slides were then stored at +4°C).

3.9. In vivo tumor imaging experiment

Initial experiments, aimed to evaluate the formation of lung tumors by the parental LLC cell line or the luciferase-transfected LLC-LUC2/1 cells, were performed by injecting cells in the lateral tail vein of recipient mice. Cells were detached using trypsin and washed twice in PBS, then resuspended in PBS and mixed in a 1:1 ratio (LLC:LLC-LUC2/1). For all injections cell concentration was 5x 10⁶/ml. Four C57BL/6 and four S376A mice were injected with 200µl (appr. 1x 10⁶ cells) of the LLC:LLC-LUC2/1 – mixture. In parallel, two control injections were performed in order to compare the tumorigenic potential of LLC-LUC2/1 with that of untransfected LLC cells. For control group 1, three C57BL/6 mice were injected with LLC cells only, whereas in control group 2 three mice were injected with LLC LUC2/1 cells only. For both groups we injected 1x 10⁶ cells in 200µl PBS. To confirm engraftment in lungs

for mice, which were injected with LLC-LUC2/1 luminescence, emission was measured one hour after injection. Mice were sacrificed 26 days post injection and lungs were analysed for the presence of tumor foci. In order to be able to monitor cancer growth *in vivo*, mice were anesthetized and luciferin had to be injected into mice intra peritoneal (IP). Luciferin serves as substrate for luciferase, triggering immediate luminescence, which can be measured by an IVIS Lumina CCD camera (Xenogen/Caliper).

4. Results

4.1.1. Activation-induced phosphorylation in SLP76-S376A knock-in mouse

T-cell stimulation triggers immediate activation of various intracellular signaling cascades. Activation-induced signaling is mainly carried out by changes in protein posttranslational modifications. Undoubtedly, the SLP76-LAT scaffold-complex plays a crucial role in TCR-dependent signal transduction, providing a platform for the recruitment of several downstream effectors of T-cell signaling (Koretzky et al., 2006).

Based on our previous work on human T-cell lines and primary T-cells, we expected that expression of the SLP76-S376A mutant would drive increased signaling and activation in T-cells from knock-in mice compared to control T-cells from C57Bl/6 mice. To test this prediction, we first decided to monitor phosphorylation of well-known markers of activation such as the Erk1 and Erk2 protein kinases (Chow et al., 2001). Indeed, activation of these enzymes is highlighted by the phosphorylation of critical Thr and Tyr sites in the catalytic domain that can be detected by phosphospecific antibodies. For these experiments, T-cells were activated by cross-linking the TCR complex and the co-stimulatory protein CD28. This was obtained by incubating cells with biotinylated antibodies against CD3 and CD28 followed by streptavidin, which binds biotinylated proteins with high affinity, thus leading to their aggregation (Levine et al., 1997).

Changes in activation-dependent phosphorylation might indicate important differences in CD4⁺ and/or CD8⁺ T-cell activation. Regarding these effects under the perspective of a whole organism, such differences may reveal relevant physiological consequences.

In an initial set of experiments, activation-induced Erk phosphorylation was detected by flow cytometry (FCM) in cells obtained from mouse spleen (Figure 14). Relevant lymphocyte populations were identified based on their size (FSC) and granularity (SSC) features (Figure 14A) and specific staining with CD8 (Figure 14B) or CD4 (Figure 14C) antibodies, labeled with different fluorochromes. Cell fixation and permeabilization allowed us to detect intracellular Erk1/2 phosphorylation in

gated CD4- or CD8-positive cells using phosphosite-specific antibodies coupled to a third fluorochrome (Figure 14D-G). When necessary, appropriate compensations were applied during data acquisition and/or analysis to correct for the spillover emission of each fluorochrome in different spectral channels. For instance, specific phospho-ERK1/2 detection without significant increase of CD4 or CD8 signal is shown in Figure 14E and 14G.

Phospho-Erk1/2 signal was induced in cells stimulated by PMA (Figure 14E and G) or CD3/CD28 cross-linking (Figure 15) but virtually undetectable in resting cells (Figure 14D, 14F and 15).

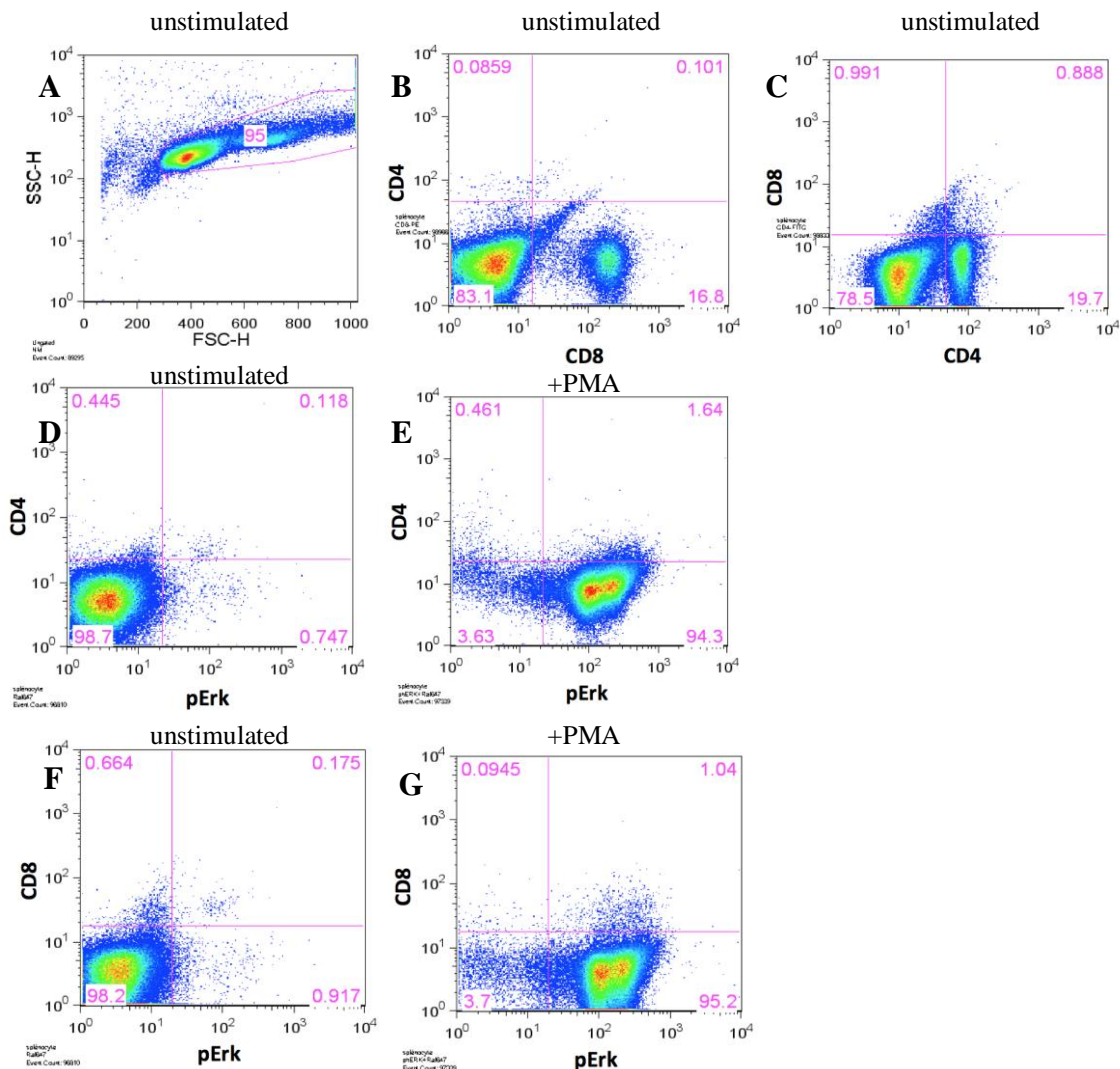


Figure 14

Flow cytometry experiment, Gating strategy. A) Selection of lymphocyte population based on size (FSC) and granularity (SSC) features, B) CD8+ T-cell analysis within the lymphocyte population gate, C)

CD4+ T-cell analysis within the lymphocyte population gate. D) Intracellular staining of ERK phosphorylation in unstimulated CD4+ T cells (negative control). E) Intracellular staining of ERK phosphorylation in PMA-treated CD4+ T cell population (positive control). F) Intracellular staining of ERK phosphorylation in unstimulated CD8+ T cells. G) Intracellular staining of ERK phosphorylation in PMA-treated CD8+ T cells.

Erk phosphorylation in CD4+ and CD8+ T-cells is shown as histograms in Figure 15, with each curve representing to one kinetic time point. The brown histogram at front resembles the positive control performed by stimulin cells with with PMA. Histograms allowed to rapidly appreciating the modifications in ERK phosphorylation in stimulated cells. However, plotting the geometric mean of phosho-ERK signal in Figure 16, gave a quantitative view of the differences in ERK activation between T cells from wild type C57Bl/6 (B6) mice and SLP76-S376A knock-in mice (SA). We found that ERK phosphorylation was slightly but consistently increased in both CD4+ and CD8+ T cells from SLP76-S376A knock-in mice as compared to wild-type cells. These data suggested that mutation of 14-3-3 binding site on SLP76 lead to increased TCR-dependent signalling in T cells, in agreement with our previous work.

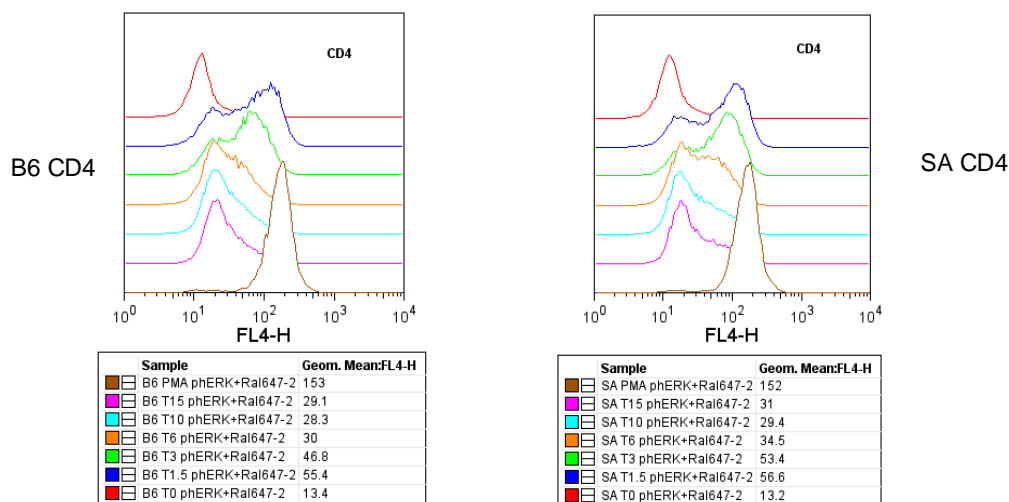


Figure 15

Flow cytometry experiment, histogram analysis of Erk phosphorylation. CD4+ T-cells were stimulated using anti-CD3 and anti-CD28 antibodies. Each histogram represents one time point of the applied kinetics, shown as follows: 0 min (*red*), 1.5 min (*blue*), 3 min (*green*), 6 min (*orange*), 10 min (*light blue*), 15 min (*pink*). Histogram for PMA positive control is shown in *brown*. C57BL/6 mice (B6) are shown on the left panel and SLP76-S376A mutant mice (SA) on the right panel.

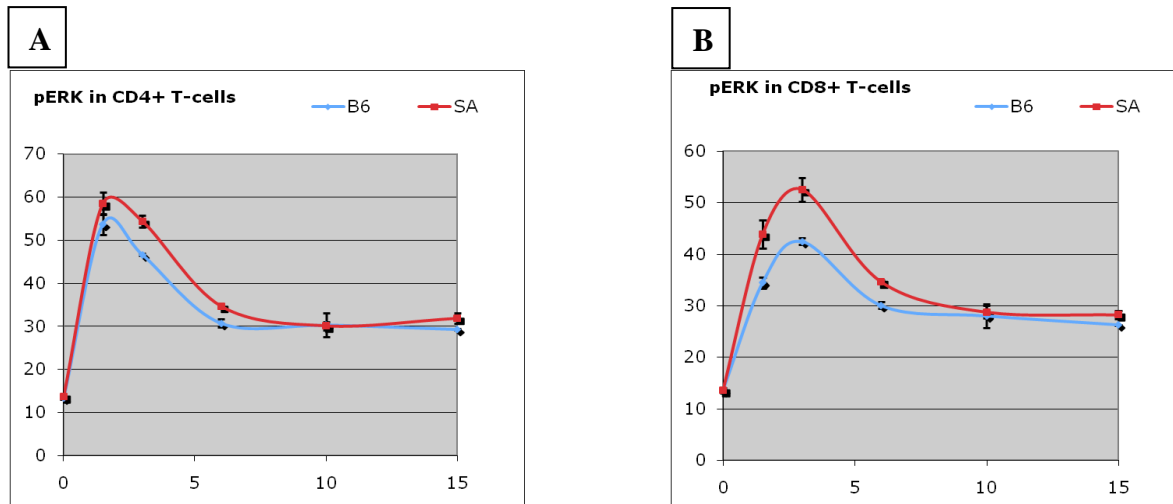


Figure 16

Flow cytometry experiment, analysis of Erk phosphorylation. Erk phosphorylation kinetic curves are shown in *blue* for C57BL/6 mice (B6) and in *red* for SLP76-S376A mutant mice (SA). CD4+ T-cells are shown on the left panel (A) and CD8+ T-cells on the right panel (B). Stimulation was performed as mentioned in Figure 15. Time of stimulation is indicated on the x-axis whereas the y-axis indicates the geometric mean .

4.1.2. Analysis of SLP76 and ERK phosphorylation by western blotting

In order to confirm the results obtained by FCM using an alternative approach, we analyzed activation-induced phosphorylation of ERK kinases using Western Blot as readout. For these experiments, we purified CD4+ and CD8+ T-cells from a pool of mouse splenocytes and lymph node cells to increase the total cell recovery. In parallel to ERK phosphorylation, we also analyzed SLP76 tyrosine phosphorylation. Indeed, we previously showed that Jurkat cells, phosphorylation of residue Y128 was increased when SLP76-S376A was expressed in Jurkat cells (Di Bartolo et al., 2007), Intensity of phosphorylated ERK and SLP76 bands was quantified and data were normalized by the amount of 14-3-3 in each lane. In some experiments, tubulin amount was used as a loading control for normalization, with identical results (data not shown). Representative western blots are shown for CD4+ and CD8+ T-cells in Figure 17. The graphs in Figure 18 and 19 show a comparison of the quantified values in either cell type from C57Bl/6 wild-type mice and SLP76-S376A mice. Concerning Erk, an increase in phosphorylation was observed in both CD4+ and CD8+ T cells from SLP76-S376A knock-in mice compared to controls (Fig. 18). These results were in line with our FCM experiments (see Fig. 16) although slight differences in the phosphorylation kinetics were sometime apparent when comparing the two techniques. On the contrary, the results concerning SLP76 (Y128)

phosphorylation (Fig. 19) were less consistent between experiments. We obtained different results in CD4+ and CD8+ T cells. Indeed, at late time points (5 and 10 minutes) SLP76 phosphorylation appeared to be stronger in SLP76-S376A cells compared to control CD4+ T cells. On the other hand, for CD8+ T-cells there was an increase of SLP76 (Y128) phosphorylation in wild-type mice compared to the mutant. We do not know whether these discrepancies are due to technical issues or to difference between these two cell types. Nonetheless, these results differ from our previous observation in Jurkat cells (see above) suggesting possible differential effects of S376 mutation in mouse vs human T cells. Further experiments are required to address these points.

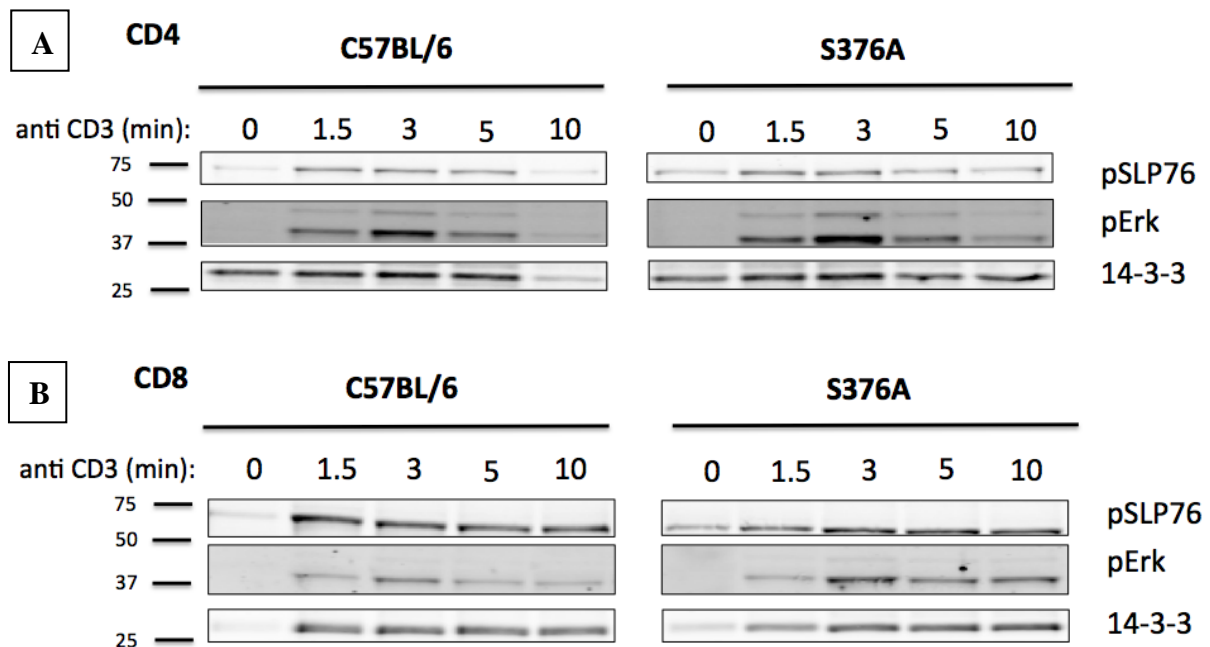


Figure 17

Western blot analysis of Erk and SLP76 phosphorylation. Wild type (C57BL/6) and SLP76-S376A (S376A) mutant CD4+ and CD8+ T-cells were stimulated using anti-CD3 and anti-CD28 antibodies. CD4+ T-cells are shown in the upper panel (A) and CD8+ T-cells in the lower panel (B). Stimulation kinetics: 0 min, 1.5 min, 3 min, 5 min, 10 min. 14-3-3 protein was used as total protein amount control.

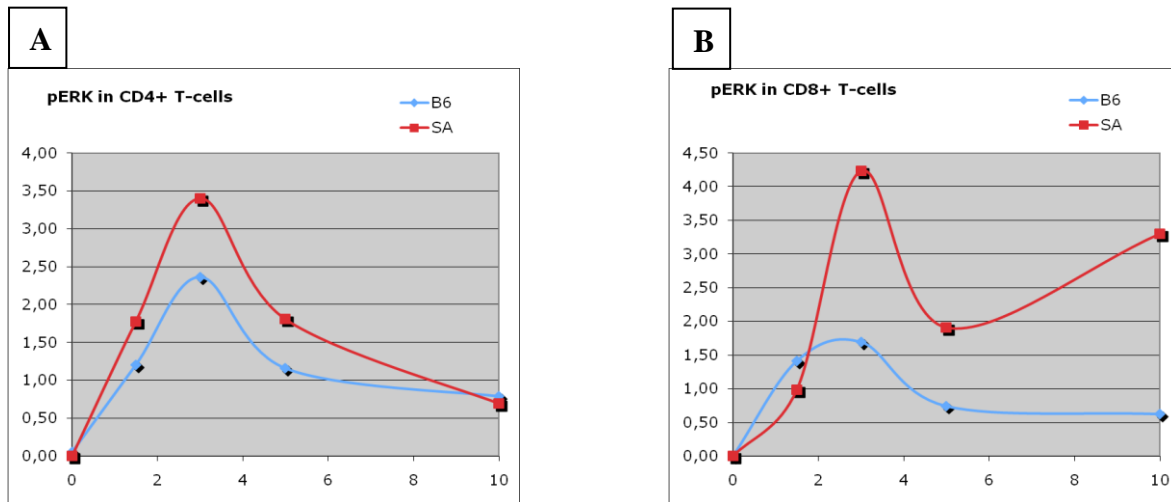


Figure 18

Quantification of Erk phosphorylation kinetics by Western blot. Wild type (*light blue*) and SLP76-S376A mutant (*red*) CD4+ and CD8+ T-cells were stimulated using anti-CD3 and antiCD-28 antibodies. CD4+ T-cells are shown in the left panel (A) and CD8+ T-cells in the right panel (B). Stimulation kinetics: 0 min, 1.5 min, 3 min, 5 min, 10 min. pErk data were normalized by the amount of 14-3-3 protein in the same sample. (see Fig. 17).

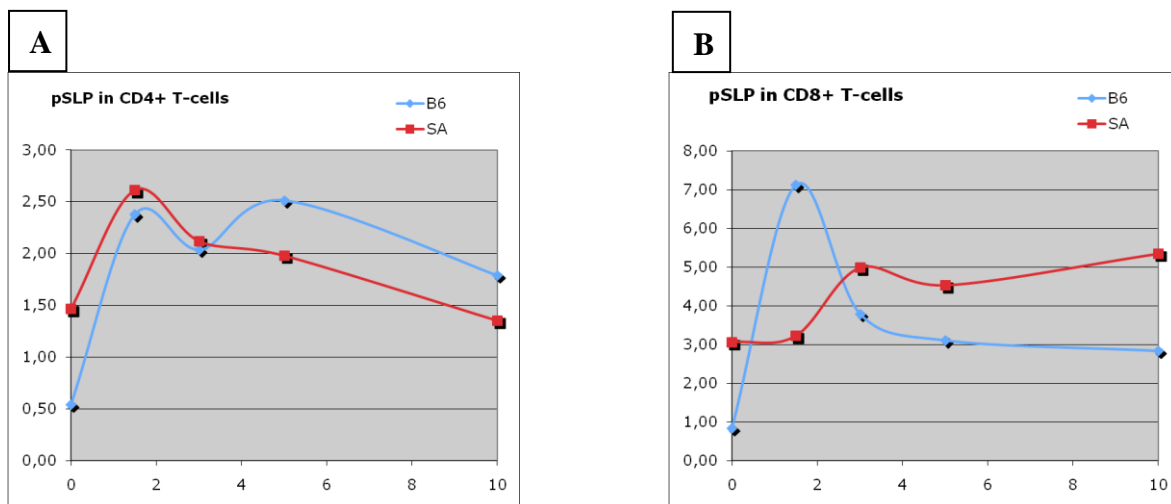


Figure 19

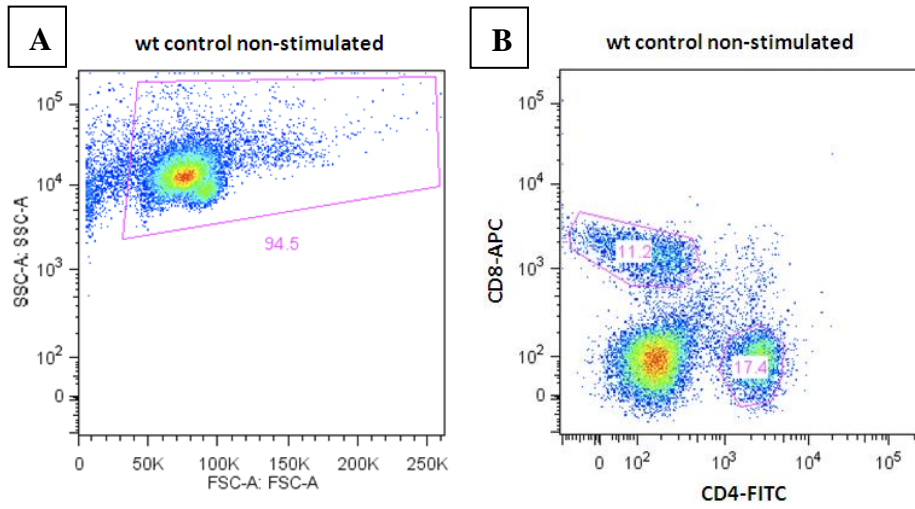
Quantification of SLP76 Y128 phosphorylation kinetics by Western blot. Wild type (*light blue*) and SLP76-S376A mutant (*red*) CD4+ and CD8+ T-cells were stimulated using anti-CD3 and anti-CD28 antibodies. CD4+ T-cells are shown in the left panel (A) and CD8+ T-cells in the right panel (B). Stimulation kinetics: 0 min, 1.5 min, 3 min, 5 min, 10 min. pSLP76 data were normalized by the amount of 14-3-3 protein in the same sample. (see Fig. 17).

4.2. Cytokine production upon activation of lymph node cells

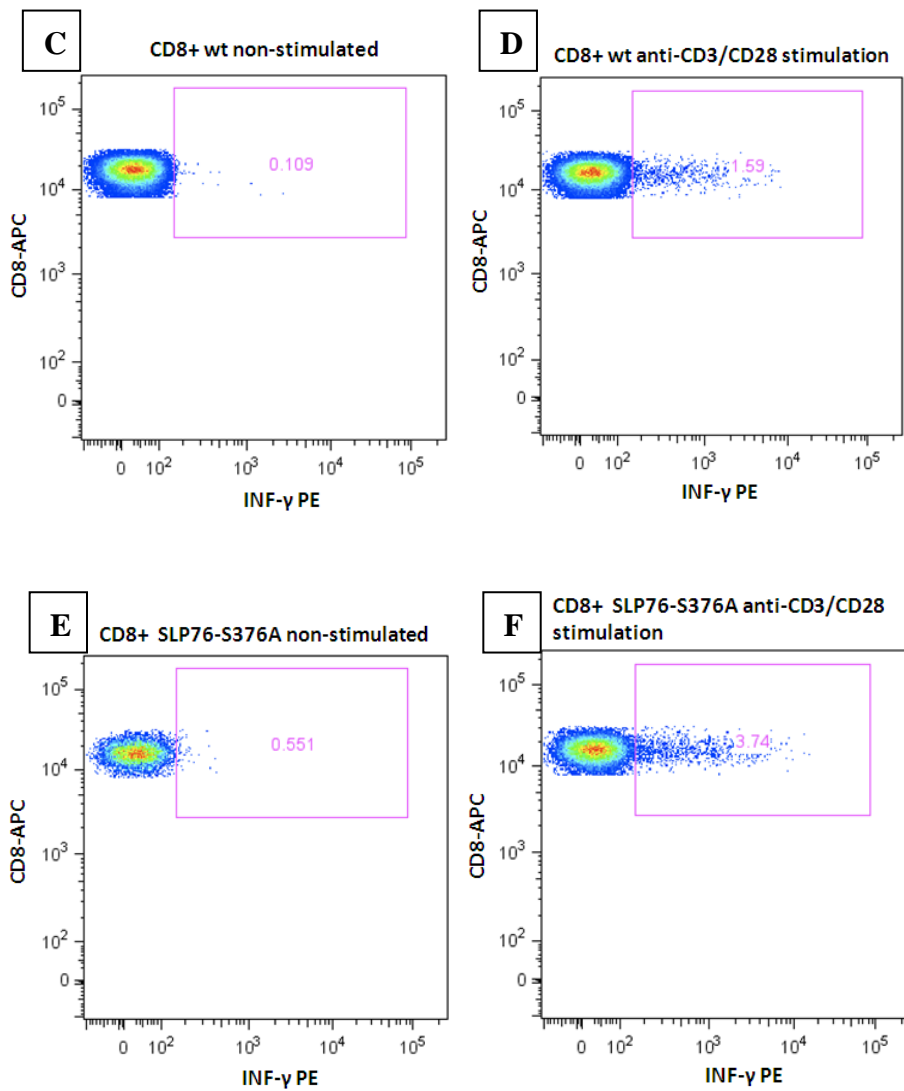
In paragraph 4.1., we focused our investigation to changes observed in early activation events. The observed increase in ERK phosphorylation in cells expressing SLP76-S376A might affect several T-cell functions, e.g. gene expression, cell communication, survival, proliferation and maturation (Roovers and Assoian, 2000). In order to verify whether this was the case, we compared the activation-induced production of cytokines by lymph node T-cells from wild type and mutant mice. Cells were prepared and stimulated for 6 hours as mentioned in paragraph 3.7.2. . Subsequent CD8 and CD4 receptor surface staining coupled to INF- γ or IL-2 intracellular staining enabled us to observe activation-induced and population-specific expression of these cytokines. Our gating strategy, SSC/FSC- and CD8/CD4 dot plots for INF- γ and IL-2 detection experiments, are shown in Figure 20A and B.

Regarding T-cells, INF- γ is known to be produced by CD4+ type 1 helper (Th1) cells and cytotoxic CD8+ T-cells (Bogen et al., 1993; Ghanekar et al., 2001) and has antiviral, immunoregulatory, and anti-tumor properties. On the other hand, IL-2 is expressed by different CD4+ and CD8+ T-cell subsets and affects T-cell growth and differentiation (Kish et al., 2005; Smith, 1988). As shown in Figure 20C-F, there was a striking increase of INF- γ production by CD8+ T-cells from SLP76-S376A mutant mice, compared to C57Bl/6 wild type animals. The comparison between wild type and mutant CD4+ T-cells suggested no significant differences concerning IL-2 production as presented in Figure 20G-J. Taken together, this data suggests a possible CD8+ T-cell specific effect for the SLP76-S376A mutant concerning INF- γ cytokine production. Given the role of IFN- γ in cellular responses, the observed two-fold increase in INF- γ secretion by SLP76-S376A CD8+ T cells is potentially relevant for anti-tumor and/or anti-viral immunity (Barth et al., 1991; Guidotti et al., 1999). This hypothesis needs to be addressed in future experiments.

Gating strategy:



CD8 INF- γ



CD4 IL-2

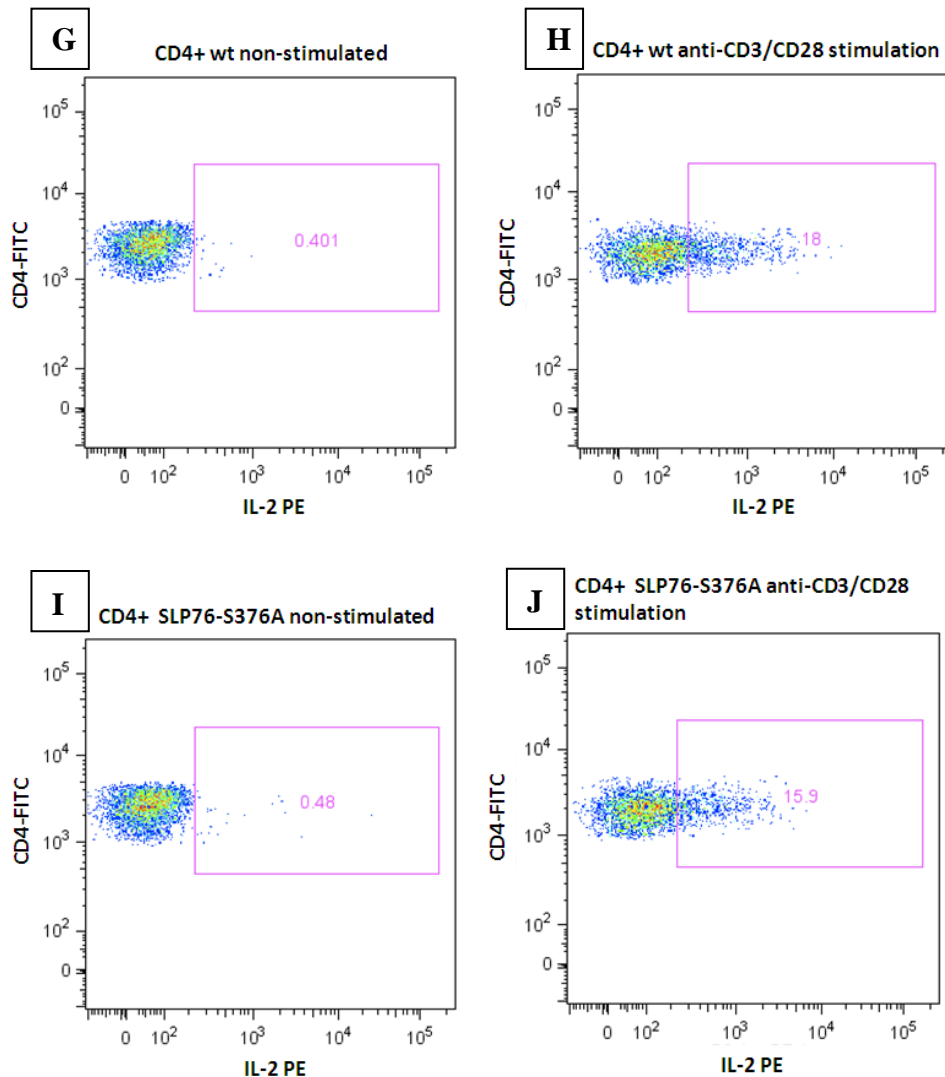


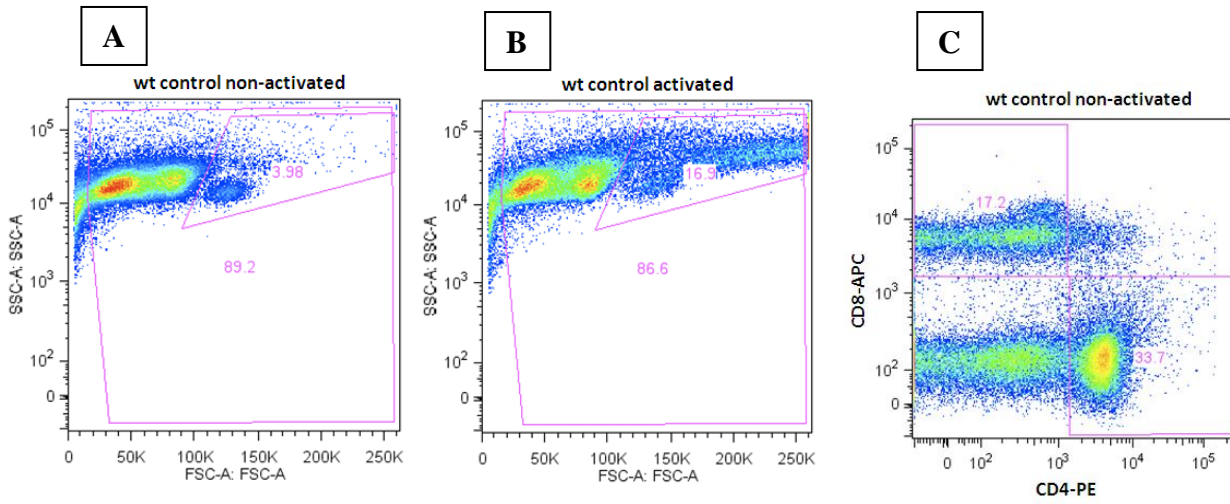
Figure 20

Flow cytometry analysis of cytokine (IL-2 and INF- γ) production. A) Gating of lymphocyte population based on FSC/SSC features, B) Selection of CD4+ and CD8+ T-cells within the lymphocyte population gated in A. C) Intracellular INF- γ staining of unstimulated wild type CD8+ T-cells (negative control). D) Intracellular INF- γ staining of wild type CD8+ T-cells upon anti-CD3/CD28 stimulation E) Intracellular INF- γ staining of unstimulated SLP76-S376A mutant CD8+ T-cells F) INF- γ intracellular staining of SLP76-S376A mutant CD8+ T-cells upon anti-CD3/CD28 stimulation G) Intracellular IL-2 staining of unstimulated wild type CD4+ T-cells. H) Intracellular IL-2 staining of wild type CD4+ T-cells after anti-CD3/CD28 stimulation I) Intracellular IL-2 staining of unstimulated SLP76-S376A mutant CD4+ T-cells IL-2 production. J) Intracellular IL-2 staining of SLP76-S376A mutant CD4+ T-cells after anti-CD3/CD28 stimulation.

4.3. T-cell proliferation assay

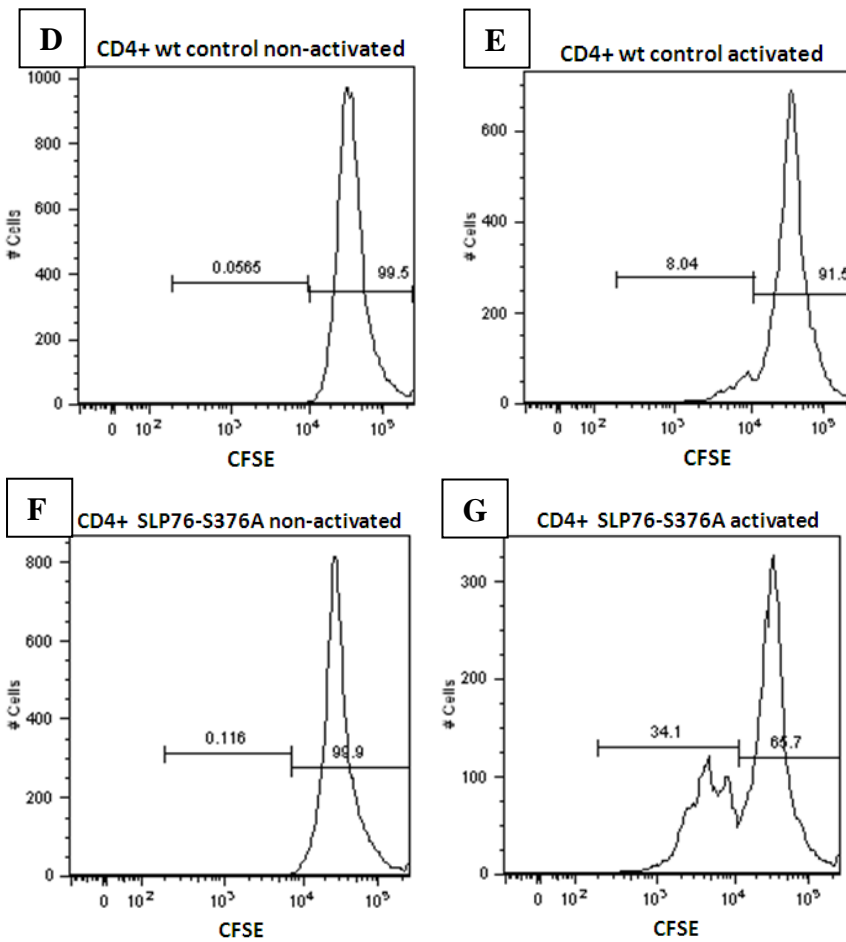
This experiment was performed to assess proliferation rate of CD4⁺ and CD8⁺ T-cells, in C57BL/6 compared to SLP76-S376A mutant mice. Interestingly, T-cells show increased proliferation in the HPK1 knockout mice (Shui et al., 2007). To test if SLP76-S376A mutant mice have a similar phenotype, we performed a CFSE-based proliferation assay (as mentioned in 3.7.3.) using lymph node (LN) cells. LN cells of C57BL/6- and SLP76-S376A-mice were isolated and stained with CFSE. Subsequently, LN cells were activated on anti-CD3 + anti-CD28 pre-coated plates for 72 hours. Non-stimulated control cells for both mutant and wild type were kept in culture medium without stimulatory antibodies. Thereafter, LN cells were stained with antibodies directed against CD4- and CD8 receptors to allow further cell proliferation analysis of these two populations by flow cytometry. Figure 21A-C shows the gating strategy; Figure 21C refers to the whole population gate and not to the blast cell gate. CFSE is a protein-labeling agent, which is detectable by flow cytometry. In each proliferation cycle the cells synthesize new proteins, thus, diluting CFSE-labeled proteins. Conversely, non-activated control cells do not divide; hence they exhibit a high CFSE signal, as shown in histograms in Figures 21D, F, H and J for wild type and mutant, respectively. Activation of T-cells triggers their proliferation therefore CFSE signal decreases with every proliferation cycle, as shown in Figures 21E, G, I and K for wild type and mutant, respectively. The bars in Figures 21D-K indicate the percentage of non-proliferating and proliferating cells. Evidently, there is a higher percentage of proliferating CD4⁺ and CD8⁺ mutant T-cells compared to wild type. This difference was more evident when the analysis was performed by gating on blast cells (e.g. activated cells with increased size), as shown in Figure 22A and B. Interestingly, this analysis reveals that a fraction of mutant T-cells performed at least an additional proliferation cycle compared to wild type T-cells. In conclusion, this assay demonstrates increased T-cell proliferation for the SLP76-S376A mutant.

Gating strategy



CFSE dilution assays

CD4+ T-cells



CD8+ T-cells

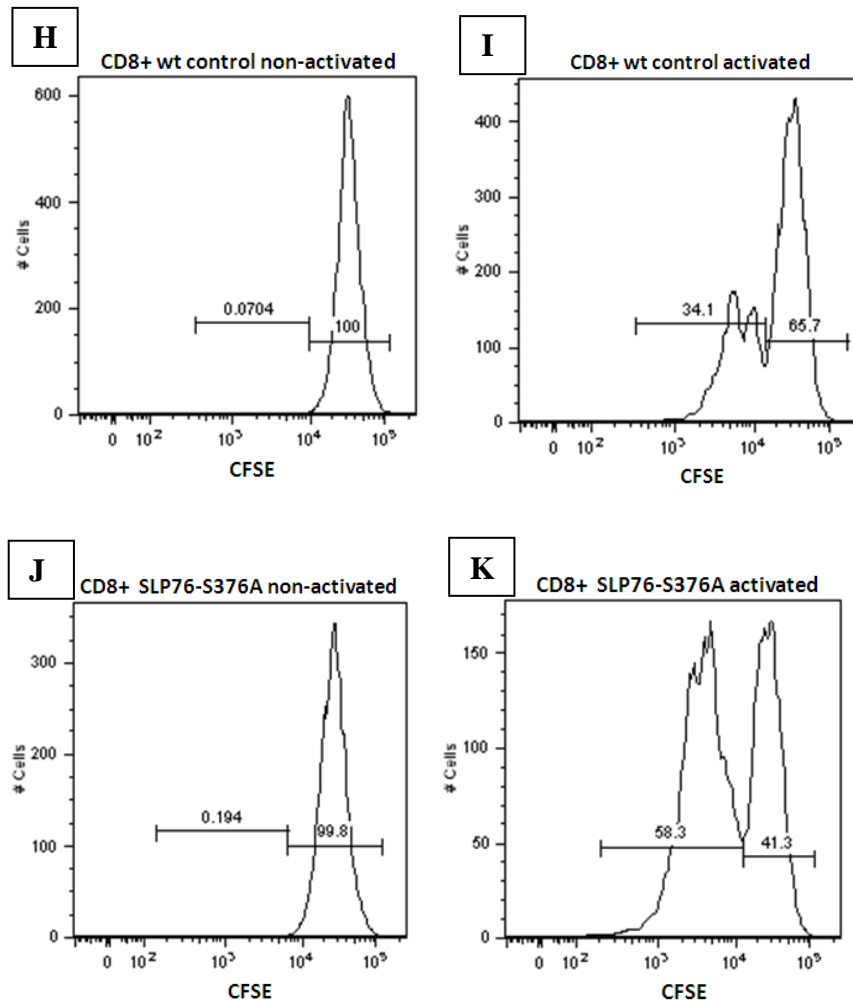


Figure 21

Analysis of lymph node T-cell proliferation by CFSE dilution assay. A. Gating on whole lymph node cell population (outer pink region) or on blast (higher size) cells (inner pink region) in non-stimulated wild type control, B. Whole cell and blast gating in stimulated wild type lymph node cells, C. Selection of CD4+ and CD8+ T-cell population within the total lymphocyte population. D to K. Histograms showing CFSE labeling of the following gated cell populations: unstimulated, wild type CD4+ T-cells (D); activated wild type CD4+ T-cells (E); unstimulated SLP76-S376A CD4+ T-cells (F); activated SLP76-S376A CD4+ T-cells (G); unstimulated wild type CD8+ T-cell (H); activated wild type CD8+ T-cells (I); unstimulated SLP76-S376A CD8+ T-cells (J); activated SLP76-S376A CD8+ T-cells (K). The percentage of not dividing vs proliferating cells (defined by the left and right black bars, respectively) is indicated in each graph.

CFSE dilution assays analysis by gating on blast cell population

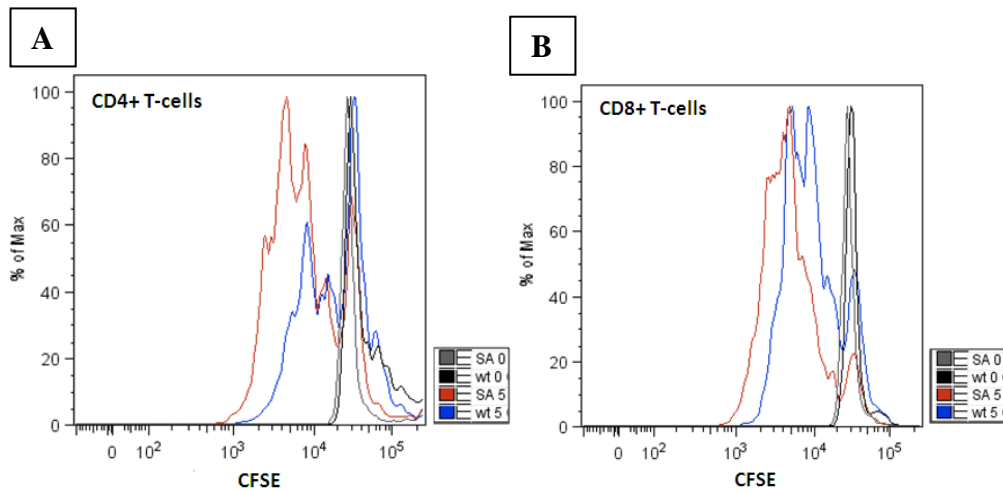


Figure 22

Analysis of T-cell proliferation by CFSE dilution assay on gated T-cell blast. CD4+ and CD8+ T-cells blasts were gated as shown in Fig. 21. CFSE signal of wild type and SLP76-S376A mutant T-cells is represented in histograms. CD4+ T-cells are shown in the left panel (A) and CD8+ T-cells in the right panel (B). Activated wild type and SLP76-S376A mutant T-cells are shown in *blue* and *red*, respectively. Non-activated wild type and SLP76-S376A mutant T-cells are shown in *black* and *grey*, respectively.

4.4. T-cell development in SLP76-S376A knock-in mice

Concerning T-cell development, in SLP76-deficient mice a maturation arrest at the double negative stage has been reported, rendering these mice devoid of mature T-cells (Clements et al., 1999). Thus, SLP76 plays an important role in T-cell development. For this reason, we conducted an analysis of T-cell maturation.

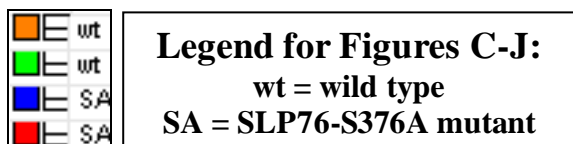
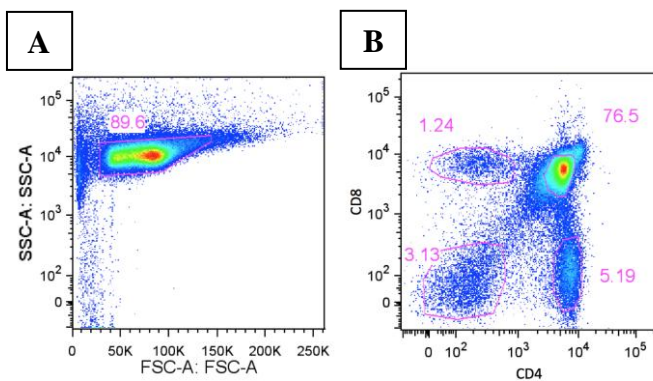
First, we analyzed the frequency of the major thymus specific sub-populations, namely double negative (DN)-, CD4 positive (CD4 pos)-, CD8 positive (CD8 pos)-, and double positive (DP) cells. A statistical analysis of wild type and SLP76-S376A knock-in mice revealed no significant differences.

We then stained thymocytes with specific surface markers, which are differentially expressed during T-cell development. CD3-receptor expression is gradually increased as a T-cell matures, whereas CD24 surface expression decreases as T-cells advance in their maturation process (Bonifacino et al., 1990;

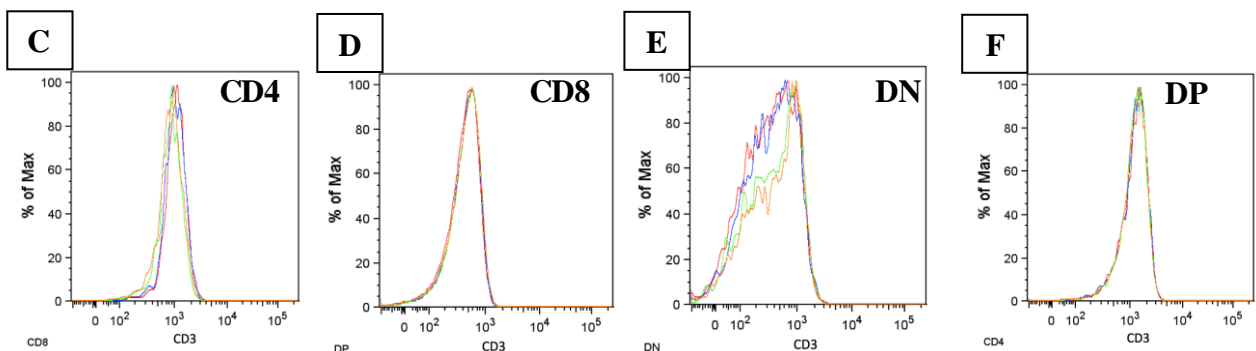
Kay et al., 1991). Additionally, CD4- and CD8 receptor labeling enabled us to monitor CD3 and CD24 expression in the four thymic sub-populations mentioned above.

Figure 23A and B represent a thymus lymphocyte population in an SSC/FSC dot plot and after CD4/CD8-labeling, respectively. For each sub-population (CD4 pos, CD8 pos, DN and DP), expression of CD3 is indicated in a histogram in Figure 23 (C-F) and for CD24 in Figure 23 (G-J). Despite occasional variations in the DN population, in summary no significant differences were observed in mutant mice concerning these markers. These results are in accordance with observations made for T-cell development in the HPK1 knockout mice, where no alterations have been described.

Gating strategy:



CD3 expression



CD24 expression

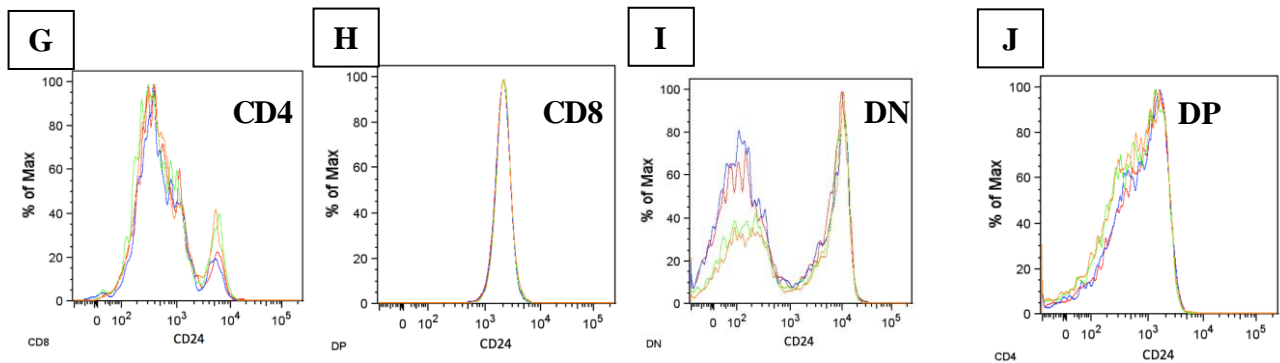


Figure 23

Analysis of expression of T-cell developmental markers, CD3 and CD24, by flow cytometry.

A. Gated thymocyte population; B. Selection of CD4+, CD8+, DN and DP T-cell population within the thymocyte population shown in A. C-J. The expression of CD3 as well as of CD24 is represented in histograms; *orange* and *green* lines indicate expression of either marker in wild type samples, whereas *blue* and *red* indicate expression in SLP76-S376A thymocytes. CD3 expression is shown for the following thymic subpopulations: CD4+ cells (C); CD8+ cells (D); DN cells (E); DP cells (F). CD24 expression is shown for the following thymus subpopulations: CD4+ cells (G); CD8+ cells (H); DN cells (I); DP cells (J).

4.5. Confocal microscopy experiments to detect possible alterations of microcluster formation in SLP76-S376A mice

The aim of this experiment was analyzing the effect of the S376A mutation on the assembly of signaling MCs and their stability in mouse T-cells. Using human T-cell lines and primary T-cells, the laboratory has previously shown that this mutation increases the stability of MCs. Indeed, based on the proposed model, phosphorylation by HPK1 and 14-3-3 binding to SLP76 would be abolished by mutating S376, thus leading to a stabilization of SLP76 binding to pLAT-containing MCs (Lasserre et al., 2011).

Purified CD4+ or CD8+ T-cells were activated by incubation on glass coverslips, pre-coated with anti-CD3 and anti-CD28 antibodies. Engagement of T-cells with these stimulatory antibodies would mimic an interaction between a T-cell and an APC, which allows visualizing of signaling MCs with high spatial resolution. MC formation has been monitored at various time points up to 7 minutes of stimulation. MCs could be visualized by immune-fluorescence staining of MC-

integrated proteins, which can then be detected by confocal microscopy. Hence, antibodies directed against pSLP76 and pLAT (two major components of MCs), were used to visualize MC-formation.

Quantification of MCs was performed using a script written using the “Acapella High Content Imaging And Analysis Software”. This script allows an automated quantification of the number of MCs per cell and their signal-intensity (Figure 25). Statistical analysis of quantification was carried out by performing an unpaired student t-test (confidence intervals 95%), using Prism (GraphPad Software, Inc. USA). Unfortunately, due to a cross-reactivity of the secondary antibody used to detect anti-pSLP76 antibody (raised in mouse) with the activating anti-CD3 antibody (raised in Armenian hamster), a high background was observed all over the surface of pSLP76-labeled coverslips (data not shown).

Figure 24A and B show the number of pLAT-containing MCs in CD4⁺ and CD8⁺ T-cells, respectively. A significant increase in the number of MCs per cell was found in mutant CD4⁺ T-cells; however no significant differences were obtained for CD8⁺ T-cells. In agreement with our hypothesis, these results suggest a higher MC stability in mutant CD4⁺ T-cells. Unexpectedly, this was not the case for the CD8⁺ T-cell population, where MCs of wild type and mutant seem to be equally stable. However, CD8⁺ T-cells appeared to be smaller and in lower abundance than CD4⁺ T-cells, therefore, changes in the acquisition or analysis settings may be required. Moreover, cell activation protocols are established for a CD4⁺ Jurkat cell line, hence, adjustments for efficient activation of CD8⁺ T-cells on coverslips might be necessary. Further experiments are needed to verify this apparent lack of effect of S376 mutation on MCs stability in CD8⁺ T-cells.

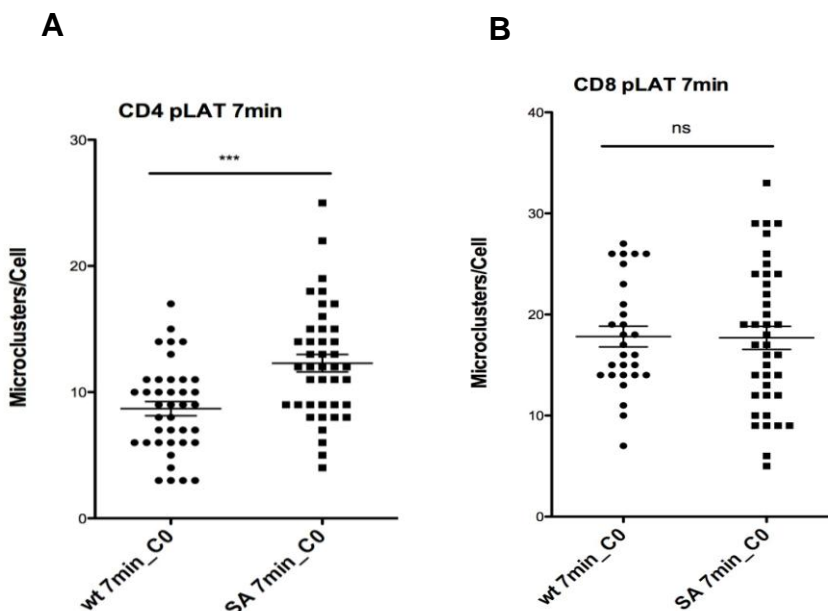


Figure 24

Analysis of signaling protein microclusters by confocal microscopy.

Each plot shows the number of pLAT microclusters per cell of either wild type or SLP76-S376A mutant, as

indicated on the X-axis. A. pLAT microclusters in CD4+ T-cells stimulated for 7 minutes. B. pLAT microclusters in CD8+ T-cells stimulated for 7 minutes. Statistical analyses showed a significant increase in the number of pLAT microclusters/cell in mutant CD4+ T-cells compared to wild-type controls (A), whereas no significant difference was observed for CD8 T-cells.

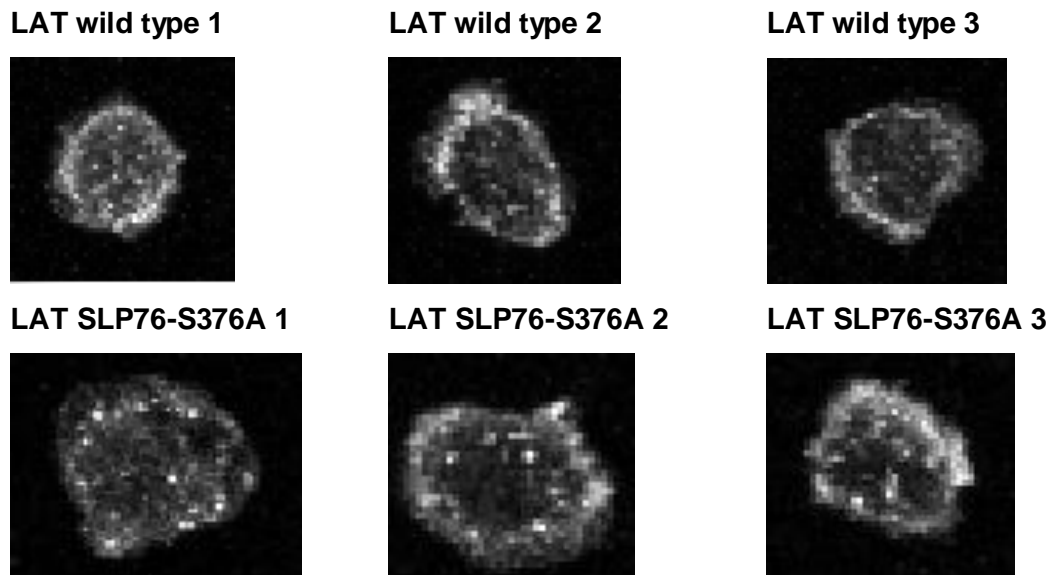


Figure 25

Microcluster imaging in CD4+ T-cells. Upper panels (LAT wild type 1,2,3) show three example images of wild type CD4+ T-cells stimulated for 7 minutes. Lower panels (LAT SLP76-S376A 1,2,3) shows three example images of wild type CD4+ T-cells stimulated for 7 minutes. A slight but significant increase in microclusters per cell for SLP76-S376A mutant T-cells is visible. For preparation of sample images shown in this figure we used **Image J** (Ref: Abramoff, M.D., Magalhaes, P.J., Ram S.J. "Image Processing with Image J". Biophotonics International volume 11, issue 7, pp. 36-42.2004) software.

4.6. Set-up of *in vivo* tumor growth imaging

This experiment was set up to determine if disruption of the 14-3-3-SLP76- interaction is involved in T-cell mediated tumor rejection.

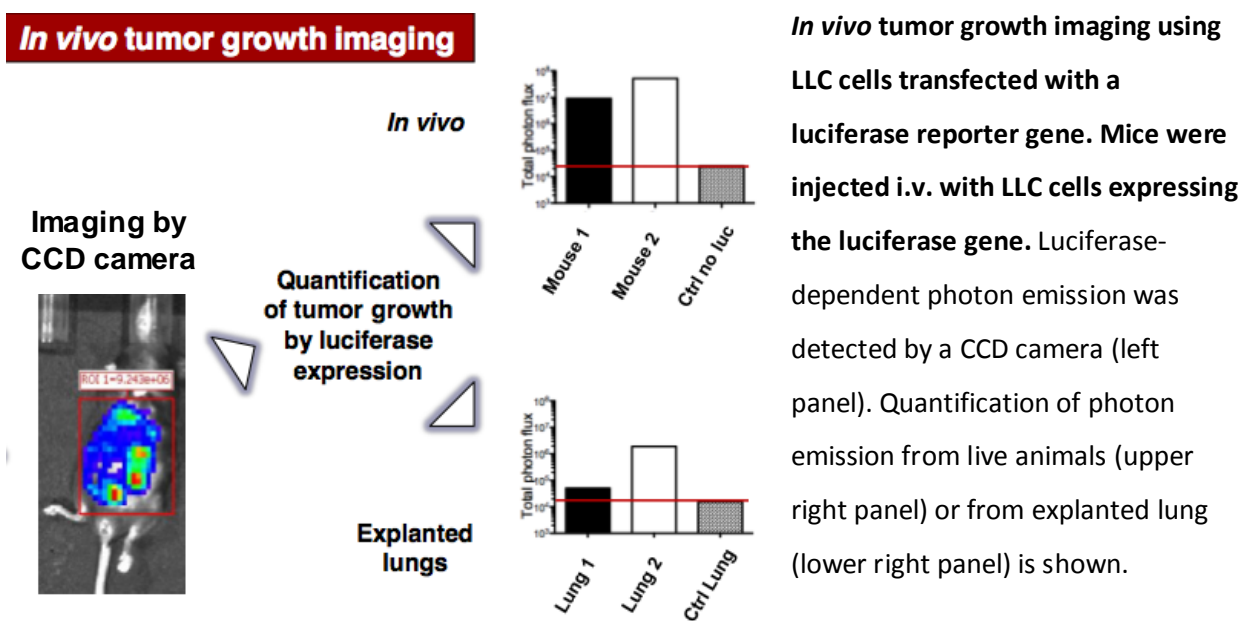
Lewis lung carcinoma (LLC) cells form lung tumors in mice. However, HPK1 knockout mice have been reported to reject tumors when challenged with LLC (Alzabin et al., 2010). HPK1 triggers a negative feedback loop shutting down T-cell activation. As explained previously, a putative mechanism involves phosphorylation of SLP76 at S376 by HPK1 and consequent binding of 14-3-3 proteins to SLP76 (Lasserre et al., 2011; Shui et al., 2007). As explained above, this interaction would

lead to disassembly of SLP76 containing signaling microclusters, thus inhibiting T-cell activation. Hence, disruption of this negative feedback loop increases T-cell activation, as demonstrated in Jurkat cells.

We decided to exploit the SLP76-S376A knock-in mice to address whether disruption of the HPK1-dependent binding of 14-3-3 proteins to SLP76 may alter the ability of CD8+ T-cells to reject LLC tumors. To this aim, we generated LLC-LUC2/1 cells, a clone of LLC transfected with a luciferase reporter vector, allowing for easier detection of tumor cells *in vivo*. To test the suitability of this experimental model, we conducted pilot experiments by injecting LLC-LUC2/1 cells in wild-type mice. Mice were monitored for 30 days. Administering luciferin by intraperitoneal injection allowed visualizing tumors immediately in anesthetized mice. Luciferase-dependent photon emission was detected (Figure 26, left panel) and quantified (Fig. 26, upper right panel) by a CCD camera. These data showed the presence of luminescent tumor cells in chest and/or abdomen of LLC-LUC2/1-injected mice but not control animals receiving non-transfected tumor cells. Subsequently, lungs were explanted and incubated with luciferin *in vitro*. Imaging with the CCD camera demonstrated the presence on luminescent tumor cells in the lungs of LLC- LUC2/1-injected but not control mice (Fig. 26, lower right panel). However, tumor growth was also detected in spleen and intestine of these animals (data not shown).

Although the presence of tumor growth outside the lungs was unexpected, these data demonstrate that the LLC-LUC2/1 cell line constitutes a valuable tool to study tumor development and anti-tumor immune responses in mice.

Figure 26



In vivo tumor growth imaging using LLC cells transfected with a luciferase reporter gene. Mice were injected i.v. with LLC cells expressing the luciferase gene. Luciferase-dependent photon emission was detected by a CCD camera (left panel). Quantification of photon emission from live animals (upper right panel) or from explanted lung (lower right panel) is shown.

5. Discussion

The initial aim of this work was to characterize T-cell development and function in SLP76-S376A knock-in mice. Based on previous results of the laboratory, this mutation was expected to result in increased TCR-dependent signaling that may potentially alter thymic development and/or peripheral T-cell responses. (Di Bartolo et al., 2007; Lasserre et al., 2011)

The work performed during my Master thesis suggests that the SLP76-S376A does not induce major changes in thymic T-cell development. For instance, my experiments demonstrated equal distribution of thymus subpopulations (DN, DP, CD8+ and CD4+) in wild type and mutant mice. Furthermore, analysis of expression of developmental markers, such as CD3 and CD24, revealed no significant changes in T-cell development. In order to detect possible defects concerning early thymocyte maturation, we used CD25 and CD44 as markers for dissecting the development of DN populations (DN1, DN2, DN3 and DN4). So far, this analysis has not revealed significant differences between control and mutant mice (data not shown). Despite no proven significance, we noticed in some experiments slight differences in CD3 and CD24 expression, especially regarding the DN population. It is unclear whether these differences reflect variability in marker expression between individual animals or are consequences of the expression of SLP76-S376A. Therefore, we plan to repeat these experiments in order to verify and support our statistical analysis. Further analyses will be performed after crossing the SLP76-S376A mice with TCR-transgenic mice that may unmask slight effects on thymic development induced by the mutation. Other described developmental markers, e.g. NUR77, whose expression is dependent on the strength of TCR signaling (Cunningham et al., 2006), will be used to further define possible developmental aberrations.

I also conducted experiments to analyze signaling and functional responses by mature T-cells. Erk-1 and -2 MAP-kinases phosphorylation is a known marker of T-cell activation. Lack of phosphorylation of S376 residue may result in increased ERK1/2 activation, as previously observed for HPK1-deficient T-cells (Shui et al., 2007). Our experiments provide evidence for similar findings in our SLP76-S376A mouse model. Mutant CD4+ and CD8+ T-cells, showed augmented Erk1/2

phosphorylation upon TCR stimulation, therefore indicating increased responsiveness to activation compared to wild type cells. These observations were made by flow cytometry analysis and subsequently confirmed by western blot experiments. However, analysis of other activation markers, as for instance phosphorylation of SLP76 Y128 residue, did not give so far conclusive results. Indeed, increased phosphorylation of this residue was observed when an SLP76-S376A mutant was expressed in Jurkat cells (Di Bartolo et al., 2007). Different kinetics of SLP76 Y128 phosphorylation in murine T-cells as compared to Jurkat cells and human primary T-cells might explain the differences observed in the different models. Alternatively, these apparent discrepancies may be due to the different stimulatory conditions used. Indeed, while previous experiments were performed by stimulating T cells with anti-CD3 antibodies (Di Bartolo et al., 2007), the results shown here were obtained after anti-CD3 and –CD28 antibody cross-linking, a procedure resulting in more efficient mouse T-cell activation. These potential explanations need to be addressed by further experiments. Additional investigations about other early T-cell activation markers will be also performed.

Increased TCR-dependent signaling may affect survival and proliferation of T-cells. Here, we demonstrated an increased proliferation rate for CD4+ and CD8+ mutant T-cells compared to wild type. Hence, we propose that lack of HPK1-mediated negative regulation in mutant T-cells is responsible for these differences in proliferation rates. This effect was more evident when performing the CFSE dilution analysis by gating specifically on cells with higher forward scattering, which include activated T-cells with increased size (i.e. blasts). We observed that a higher percentage of blast cells in the mutant have reduced levels of CFSE labeling compared to wild type, suggesting an increased proliferation of the former. However, we cannot rule out that these data reflect an increased resistance of mutant T cells to activation-induced cell death (Brenner et al., 2005). Further experiments need to be performed to confirm these data and address the underlying cellular mechanism.

Cytokine production assays were performed to further explore the consequences of increased responsiveness of SLP76-S376A T-cells. We analyzed in particular the production of IL-2 and INF- γ by in vitro-stimulated control and mutant T-cells. Whereas these studies did not reveal significant differences in IL-2 production, we observed a two fold increase of INF- γ production by mutant T-cells. INF- γ is a pro-inflammatory cytokine (type 2 class Interferon), which exerts immunostimulatory

and immunomodulatory effects e.g. activation of macrophages, NK cells and cytotoxic CD8⁺ T-cells (Schroder et al., 2004). NK cells and cytotoxic CD8⁺ T-cells are effector cells important for anti-tumoral and anti-viral activity. Hence, increased production of INF- γ by T-cells may improve multiple functions of these cells and boost immune responses. It will be interesting to determine whether INF- γ production is increased in other hematopoietic cell types (e.g. NK cells) that also express SLP76 and to define the functional consequences of this modification on immune responses. These results suggest that SLP76-S376A expression induce a specific effect on INF- γ production, although it is currently unclear how the mutation of SLP76 may affect signaling pathways controlling IFN- γ but not IL-2 production. IL-2 is important for T-cell development but also for survival, proliferation, growth and differentiation of T-cells (Boyman and Sprent, 2012). Thus, further experiments will have to be performed to confirm this data and possibly investigate the molecular control of selective cytokine production by SLP76.

Altogether, the functional modifications detected in SLP76-S376A T-cells are reminiscent of the phenotype displayed by HPK1 knockout mice. HPK1-deficient T-cells show a higher proliferation rate, as well as augmented IL-2 production (Shui et al., 2007). Interestingly, an inverse correlation between HPK1 expression and INF- γ production has been reported for human CD4⁺ T-cells (Zhang et al., 2011). To our knowledge, the effect on INF- γ production has not yet been described in HPK1 knock-out mice. However, HPK1 deficient mice were reported to exhibit increased T-cell mediated anti-tumor activity (Alzabin et al., 2010), therefore we decided to set up a bioluminescence based assay, which would enable us to quantify tumor growth *in vivo*. This tumor growth assay was performed using LLC cells, which produce large amounts of prostaglandin E2 (PGE2). PGE2 is a naturally occurring lipid compound that among a variety of different functions also acts as regulator of inflammation (Kalinski, 2012). According to the literature, PGE2 can activate HPK1 by a cAMP-dependent pathway but the molecular mechanism of how HPK1 exerts its negative regulation of anti-tumor immunity is not well understood. We propose a model where PGE2-mediated activation of HPK1, affects T-cell activity by enforcing HPK1-mediated phosphorylation of SLP76 and negative regulation of T-cell signaling and activation. Since our mouse model is defective for this negative regulatory pathway, it is a suitable tool to challenge our model. If our hypothesis is valid, SLP76-S376A

mice should show higher resistance against the PGE2-induced immune suppressive effects.

CD8⁺ T-cells are effector cells that are able to induce apoptosis in target cells, e.g. tumor cells, by different mechanisms. PGE2-induced inhibition of T-cell activation might impede these T-cell effector mechanisms, however, on the cell biological level very little is known. The formation of a cytolytic synapse between a T-cell and a target cell is crucial for efficient target cell killing. A sequence of specific events implying TCR-signaling, recruitment and activation of adhesion molecules, cytoskeleton rearrangements, eventually leads to secretion of cytotoxic granules and apoptosis induction (Jenkins and Griffiths, 2010). Interestingly, both HPK1 and SLP76 may modulate several of these events (Koretzky et al., 2006; Patzak et al., 2010; Shui et al., 2007). Moreover, Erk phosphorylation has been implicated in regulating the delivery of cytolytic granules to the cytolytic synapses (Chen et al., 2006). As mentioned above, HPK1 as well as our SLP76-S376A mutant show higher levels of Erk phosphorylation that, in principle, might affect the formation of a cytolytic synapse. This hypothesis may be addressed by conducting further confocal microscopy experiments. It will be interesting to address whether PGE2 may affect cytolytic synapse formation and/or function by altering the pathways mentioned above.

LCK as well as ZAP70 are essential tyrosine kinases involved in early TCR-signaling. Their activity also contributes to efficient cytolytic synapse formation. LAT and SLP76 are two major scaffold proteins of signaling complexes and are both substrates of ZAP70. Increased phosphorylation of these proteins and higher stability of signaling microclusters were recently demonstrated in human T cells upon HPK1 knockdown or expression of SLP76-S376A (Lasserre et al., 2011). Hence, I tried to verify whether this was also the case in mutant mice, since it could explain the observed increase in downstream signaling. Several difficulties with the set up of microcluster visualization with mouse T-cells by confocal microscopy, made it difficult to analyze obtained data. Moreover, we need to reconfirm these experiments by adding more time points to our kinetics. Nevertheless, at late stimulation time points (e.g. 7 minutes), I observed some increase in the stability of pLAT microclusters in CD4⁺ T-cells from the SLP76-S376A mice. I performed similar experiments with CD8⁺ T-cells, but no alterations of microcluster stability could be detected in this case. However, due to the reduced size of CD8⁺ T-cell compared to CD4⁺ T-cells,

detection of microclusters in the former will require further optimization. The results I obtained so far do not provide data with statistical significance; hence they need to be repeated. Possible modification of the detection settings may be of help for increasing the detection of microclusters per cell (e.g. acquiring images at higher zoom values compared to those used for CD4+ T-cells).

In summary, the results obtained so far indicate that SLP76-S376A mutant expression in mice induces no developmental alterations, whereas mutant T-cells exhibit increased signaling, higher cell proliferation rate and increased production of selected cytokines for CD8+ T-cells upon TCR induction. Moreover, the tools I generated during my Master Thesis will allow future investigations about the role of the HPK1-mediated negative regulation of T-cell activation in T-cell-dependent anti-tumor immunity. Elucidating further functions of HPK1 may eventually lead to hints for novel HPK1-targeted cancer immunotherapy (Sawasdikosol et al., 2012).

6. Bibliography

- Alzabin, S., Pyarajan, S., Yee, H., Kiefer, F., Suzuki, A., Burakoff, S., and Sawadkiosol, S. (2010). Hematopoietic progenitor kinase 1 is a critical component of prostaglandin E2-mediated suppression of the anti-tumor immune response. *Cancer immunology, immunotherapy : CII* 59, 419-429.
- August, A., and Ragin, M.J. (2012). Regulation of T-cell responses and disease by tec kinase Itk. *International reviews of immunology* 31, 155-165.
- Barth, R.J., Jr., Mule, J.J., Spiess, P.J., and Rosenberg, S.A. (1991). Interferon gamma and tumor necrosis factor have a role in tumor regressions mediated by murine CD8+ tumor-infiltrating lymphocytes. *The Journal of experimental medicine* 173, 647-658.
- Bertram, J.S., and Janik, P. (1980). Establishment of a cloned line of Lewis Lung Carcinoma cells adapted to cell culture. *Cancer letters* 11, 63-73.
- Bogen, S.A., Fogelman, I., and Abbas, A.K. (1993). Analysis of IL-2, IL-4, and IFN-gamma-producing cells in situ during immune responses to protein antigens. *J Immunol* 150, 4197-4205.
- Bonifacio, J.S., McCarthy, S.A., Maguire, J.E., Nakayama, T., Singer, D.S., Klausner, R.D., and Singer, A. (1990). Novel post-translational regulation of TCR expression in CD4+CD8+ thymocytes influenced by CD4. *Nature* 344, 247-251.
- Boomer, J.S., and Tan, T.H. (2005). Functional interactions of HPK1 with adaptor proteins. *Journal of cellular biochemistry* 95, 34-44.
- Boyman, O., and Sprent, J. (2012). The role of interleukin-2 during homeostasis and activation of the immune system. *Nature reviews Immunology* 12, 180-190.
- Brenner, D., Golks, A., Kiefer, F., Krammer, P.H., and Arnold, R. (2005). Activation or suppression of NFkappaB by HPK1 determines sensitivity to activation-induced cell death. *The EMBO journal* 24, 4279-4290.
- Bubeck Wardenburg, J., Pappu, R., Bu, J.Y., Mayer, B., Chernoff, J., Straus, D., and Chan, A.C. (1998). Regulation of PAK activation and the T cell cytoskeleton by the linker protein SLP-76. *Immunity* 9, 607-616.
- Chen, X., Allan, D.S., Krzewski, K., Ge, B., Kopcow, H., and Strominger, J.L. (2006). CD28-stimulated ERK2 phosphorylation is required for polarization of the microtubule organizing center and granules in YTS NK cells. *Proceedings of the National Academy of Sciences of the United States of America* 103, 10346-10351.
- Chow, S., Patel, H., and Hedley, D.W. (2001). Measurement of MAP kinase activation by flow cytometry using phospho-specific antibodies to MEK and ERK: potential for pharmacodynamic monitoring of signal transduction inhibitors. *Cytometry* 46, 72-78.
- Clements, J.L., Lee, J.R., Gross, B., Yang, B., Olson, J.D., Sandra, A., Watson, S.P., Lentz, S.R., and Koretzky, G.A. (1999). Fetal hemorrhage and platelet dysfunction in SLP-76-deficient mice. *The Journal of clinical investigation* 103, 19-25.
- Cunningham, N.R., Artim, S.C., Fornadel, C.M., Sellars, M.C., Edmonson, S.G., Scott, G., Albino, F., Mathur, A., and Punt, J.A. (2006). Immature CD4+CD8+ thymocytes and mature T cells regulate Nur77 distinctly in response to TCR stimulation. *J Immunol* 177, 6660-6666.
- Di Bartolo, V., Montagne, B., Salek, M., Jungwirth, B., Carrette, F., Fourtane, J., Sol-Foulon, N., Michel, F., Schwartz, O., Lehmann, W.D., *et al.* (2007). A novel pathway down-modulating T cell activation involves HPK-1-dependent recruitment of 14-3-3 proteins on SLP-76. *The Journal of experimental medicine* 204, 681-691.

- Dustin, M.L., Chakraborty, A.K., and Shaw, A.S. (2010). Understanding the structure and function of the immunological synapse. *Cold Spring Harbor perspectives in biology* 2, a002311.
- Fang, N., Motto, D.G., Ross, S.E., and Koretzky, G.A. (1996). Tyrosines 113, 128, and 145 of SLP-76 are required for optimal augmentation of NFAT promoter activity. *J Immunol* 157, 3769-3773.
- Ghanekar, S.A., Nomura, L.E., Suni, M.A., Picker, L.J., Maecker, H.T., and Maino, V.C. (2001). Gamma interferon expression in CD8(+) T cells is a marker for circulating cytotoxic T lymphocytes that recognize an HLA A2-restricted epitope of human cytomegalovirus phosphoprotein pp65. *Clinical and diagnostic laboratory immunology* 8, 628-631.
- Guidotti, L.G., Borrow, P., Brown, A., McClary, H., Koch, R., and Chisari, F.V. (1999). Noncytopathic clearance of lymphocytic choriomeningitis virus from the hepatocyte. *The Journal of experimental medicine* 189, 1555-1564.
- Hogquist, K.A., Jameson, S.C., Heath, W.R., Howard, J.L., Bevan, M.J., and Carbone, F.R. (1994). T cell receptor antagonist peptides induce positive selection. *Cell* 76, 17-27.
- Hu, M.C., Qiu, W.R., Wang, X., Meyer, C.F., and Tan, T.H. (1996). Human HPK1, a novel human hematopoietic progenitor kinase that activates the JNK/SAPK kinase cascade. *Genes & development* 10, 2251-2264.
- Hu, M.C., Wang, Y., Qiu, W.R., Mikhail, A., Meyer, C.F., and Tan, T.H. (1999). Hematopoietic progenitor kinase-1 (HPK1) stress response signaling pathway activates I κ B kinases (IKK- α / β) and IKK- β is a developmentally regulated protein kinase. *Oncogene* 18, 5514-5524.
- Ikeda, H., Old, L.J., and Schreiber, R.D. (2002). The roles of IFN gamma in protection against tumor development and cancer immunoediting. *Cytokine & growth factor reviews* 13, 95-109.
- Inoshima, N., Wang, Y., and Wardenburg, J.B. (2012). Genetic requirement for ADAM10 in severe *Staphylococcus aureus* skin infection. *The Journal of investigative dermatology* 132, 1513-1516.
- Jenkins, M.R., and Griffiths, G.M. (2010). The synapse and cytolytic machinery of cytotoxic T cells. *Current opinion in immunology* 22, 308-313.
- Kalinski, P. (2012). Regulation of immune responses by prostaglandin E2. *J Immunol* 188, 21-28.
- Kay, R., Rosten, P.M., and Humphries, R.K. (1991). CD24, a signal transducer modulating B cell activation responses, is a very short peptide with a glycosyl phosphatidylinositol membrane anchor. *J Immunol* 147, 1412-1416.
- Kiefer, F., Tibbles, L.A., Anafi, M., Janssen, A., Zanke, B.W., Lassam, N., Pawson, T., Woodgett, J.R., and Iscove, N.N. (1996). HPK1, a hematopoietic protein kinase activating the SAPK/JNK pathway. *The EMBO journal* 15, 7013-7025.
- Kish, D.D., Gorbachev, A.V., and Fairchild, R.L. (2005). CD8+ T cells produce IL-2, which is required for CD(4+)CD25+ T cell regulation of effector CD8+ T cell development for contact hypersensitivity responses. *Journal of leukocyte biology* 78, 725-735.
- Koretzky, G.A., Abtahian, F., and Silverman, M.A. (2006). SLP76 and SLP65: complex regulation of signalling in lymphocytes and beyond. *Nature reviews Immunology* 6, 67-78.
- Lasserre, R., Cuche, C., Blecher-Gonen, R., Libman, E., Biquand, E., Danckaert, A., Yablonski, D., Alcover, A., and Di Bartolo, V. (2011). Release of serine/threonine-phosphorylated adaptors from signaling microclusters down-regulates T cell activation. *The Journal of cell biology* 195, 839-853.

- Le Bras, S., Foucault, I., Foussat, A., Brignone, C., Acuto, O., and Deckert, M. (2004). Recruitment of the actin-binding protein HIP-55 to the immunological synapse regulates T cell receptor signaling and endocytosis. *The Journal of biological chemistry* 279, 15550-15560.
- Levine, B.L., Bernstein, W.B., Connors, M., Craighead, N., Lindsten, T., Thompson, C.B., and June, C.H. (1997). Effects of CD28 costimulation on long-term proliferation of CD4+ T cells in the absence of exogenous feeder cells. *J Immunol* 159, 5921-5930.
- Ling, P., Yao, Z., Meyer, C.F., Wang, X.S., Oehrl, W., Feller, S.M., and Tan, T.H. (1999). Interaction of hematopoietic progenitor kinase 1 with adapter proteins Crk and CrkL leads to synergistic activation of c-Jun N-terminal kinase. *Molecular and cellular biology* 19, 1359-1368.
- Liou, J., Kiefer, F., Dang, A., Hashimoto, A., Cobb, M.H., Kurosaki, T., and Weiss, A. (2000). HPK1 is activated by lymphocyte antigen receptors and negatively regulates AP-1. *Immunity* 12, 399-408.
- Ma, W., Xia, C., Ling, P., Qiu, M., Luo, Y., Tan, T.H., and Liu, M. (2001). Leukocyte-specific adaptor protein Grap2 interacts with hematopoietic progenitor kinase 1 (HPK1) to activate JNK signaling pathway in T lymphocytes. *Oncogene* 20, 1703-1714.
- Medeiros, R.B., Burbach, B.J., Mueller, K.L., Srivastava, R., Moon, J.J., Highfill, S., Peterson, E.J., and Shimizu, Y. (2007). Regulation of NF-kappaB activation in T cells via association of the adapter proteins ADAP and CARMA1. *Science* 316, 754-758.
- Motto, D.G., Ross, S.E., Wu, J., Hendricks-Taylor, L.R., and Koretzky, G.A. (1996). Implication of the GRB2-associated phosphoprotein SLP-76 in T cell receptor-mediated interleukin 2 production. *The Journal of experimental medicine* 183, 1937-1943.
- Mueller, K.L., Thomas, M.S., Burbach, B.J., Peterson, E.J., and Shimizu, Y. (2007). Adhesion and degranulation-promoting adapter protein (ADAP) positively regulates T cell sensitivity to antigen and T cell survival. *J Immunol* 179, 3559-3569.
- Nicolson, G.L., Brunson, K.W., and Fidler, I.J. (1978). Specificity of arrest, survival, and growth of selected metastatic variant cell lines. *Cancer research* 38, 4105-4111.
- Patzak, I.M., Konigsberger, S., Suzuki, A., Mak, T.W., and Kiefer, F. (2010). HPK1 competes with ADAP for SLP-76 binding and via Rap1 negatively affects T-cell adhesion. *European journal of immunology* 40, 3220-3225.
- Roovers, K., and Assoian, R.K. (2000). Integrating the MAP kinase signal into the G1 phase cell cycle machinery. *BioEssays : news and reviews in molecular, cellular and developmental biology* 22, 818-826.
- Samelson, L.E. (2002). Signal transduction mediated by the T cell antigen receptor: the role of adapter proteins. *Annual review of immunology* 20, 371-394.
- Sauer, K., Liou, J., Singh, S.B., Yablonski, D., Weiss, A., and Perlmutter, R.M. (2001). Hematopoietic progenitor kinase 1 associates physically and functionally with the adaptor proteins B cell linker protein and SLP-76 in lymphocytes. *The Journal of biological chemistry* 276, 45207-45216.
- Sawasdikosol, S., Pyarajan, S., Alzabin, S., Matejovic, G., and Burakoff, S.J. (2007). Prostaglandin E2 activates HPK1 kinase activity via a PKA-dependent pathway. *The Journal of biological chemistry* 282, 34693-34699.
- Sawasdikosol, S., Zha, R., Yang, B., and Burakoff, S. (2012). HPK1 as a novel target for cancer immunotherapy. *Immunologic research*.
- Schroder, K., Hertzog, P.J., Ravasi, T., and Hume, D.A. (2004). Interferon-gamma: an overview of signals, mechanisms and functions. *Journal of leukocyte biology* 75, 163-189.
- Sela, M., Bogin, Y., Beach, D., Oellerich, T., Lehne, J., Smith-Garvin, J.E., Okumura, M., Starosvetsky, E., Kosoff, R., Libman, E., *et al.* (2011). Sequential phosphorylation of

- SLP-76 at tyrosine 173 is required for activation of T and mast cells. *The EMBO journal* 30, 3160-3172.
- Shui, J.W., Boomer, J.S., Han, J., Xu, J., Dement, G.A., Zhou, G., and Tan, T.H. (2007). Hematopoietic progenitor kinase 1 negatively regulates T cell receptor signaling and T cell-mediated immune responses. *Nature immunology* 8, 84-91.
- Singer, A.L., Bunnell, S.C., Obstfeld, A.E., Jordan, M.S., Wu, J.N., Myung, P.S., Samelson, L.E., and Koretzky, G.A. (2004). Roles of the proline-rich domain in SLP-76 subcellular localization and T cell function. *The Journal of biological chemistry* 279, 15481-15490.
- Smith, K.A. (1988). Interleukin-2: inception, impact, and implications. *Science* 240, 1169-1176.
- Trautmann, A. (2005). Microclusters initiate and sustain T cell signaling. *Nature immunology* 6, 1213-1214.
- Wu, J.N., Gheith, S., Bezman, N.A., Liu, Q.H., Fostel, L.V., Swanson, A.M., Freedman, B.D., Koretzky, G.A., and Peterson, E.J. (2006). Adhesion- and degranulation-promoting adapter protein is required for efficient thymocyte development and selection. *J Immunol* 176, 6681-6689.
- Yablonski, D., Kadlecik, T., and Weiss, A. (2001). Identification of a phospholipase C-gamma1 (PLC-gamma1) SH3 domain-binding site in SLP-76 required for T-cell receptor-mediated activation of PLC-gamma1 and NFAT. *Molecular and cellular biology* 21, 4208-4218.
- Yablonski, D., Kuhne, M.R., Kadlecik, T., and Weiss, A. (1998). Uncoupling of nonreceptor tyrosine kinases from PLC-gamma1 in an SLP-76-deficient T cell. *Science* 281, 413-416.
- Young, M.R., and Knies, S. (1984). Prostaglandin E production by Lewis lung carcinoma: mechanism for tumor establishment in vivo. *Journal of the National Cancer Institute* 72, 919-922.
- Zhang, Q., Long, H., Liao, J., Zhao, M., Liang, G., Wu, X., Zhang, P., Ding, S., Luo, S., and Lu, Q. (2011). Inhibited expression of hematopoietic progenitor kinase 1 associated with loss of jumonji domain containing 3 promoter binding contributes to autoimmunity in systemic lupus erythematosus. *Journal of autoimmunity* 37, 180-189.
- Zhang, W., Sloan-Lancaster, J., Kitchen, J., Tribble, R.P., and Samelson, L.E. (1998). LAT: the ZAP-70 tyrosine kinase substrate that links T cell receptor to cellular activation. *Cell* 92, 83-92.

I would like to state clearly, that I have tried to cite my sources to the best of my knowledge. These sources are listed in the “bibliography section 6”. However, for a minor part of the introduction (subsection 2.1 and 2.2.), it shall be noted that the book “Janeway’s Immunobiology, seventh edition” was used as source.

7. Appendix

Victor Navas – Curriculum Vitae

Personal details

Date of birth: 22.05.1986 Address: Favoritenstraße 14/8, 1040 Vienna - Austria
Place of birth: Quito, Ecuador Email: vnavas@gmail.com
Nationality: Austrian Phone number: +43 680 5024 911

Education

2006 October - 2012 August (expected date of completion)

MSc in Molecular Biology, University of Vienna
Specialization in Immunology, Molecular Medicine and Cell Biology

2006 April - 2006 September

Certificate II in Information Technology, Bridge Business College Sydney

2005 July - 2006 March

Compulsory Austrian Military - Service

1996 - 2005 Secondary school, Billrothgymnasium GRW 19

School - Representative 2003 - 2004, natural science branch, Austrian Matura

1992 - 1996 Primary school, Volksschule Kreindlgasse

Working Experience

**2011 October - 2010 May, Master's Thesis
Institut Pasteur (Paris - France)**

Group Andres Alcover

Project: "The role of scaffold-protein SLP76 in a recently discovered negative feed back loop, regulating T-cell receptor activation in mice". Characterization of a SLP76-S376A knock-in mouse, by monitoring cell proliferation, cytokine production, microcluster formation and activation-induced phosphorylation of e.g.: Erk, SLP76. Methods: Flow cytometry, Western blot, Confocal microscopy

**2011 February - 2011 June, Internship (ERASMUS student exchange program)
Institut Pasteur (Paris - France)**

Group Fernando Arenzana Seisdedos

Project: "Characterization of CCR5- and CD4-receptor expression in 293 - Affinofile Cells". HEK-derived Affinofile cells comprise an antibiotics-inducible CCR5- and CD4-receptor expression system. Analysis of receptor expression levels upon different stimulation conditions, using flow cytometry. Monitoring of HIV infection efficiency depending on expression levels of CCR5 and CD4, using a luciferase reporter. Methods: Flow cytometry, cell membrane purification, viral infection of cells, cell-fusion assays

2010 October - 2011 January, Internship

Institute for Molecular Biotechnology Austria (IMBA)

Group Josef Penninger

Project: "Role of RANK/RANKL in central tolerance during pregnancy". Investigation of RANK/RANKL-mediated interaction between medullary thymic epithelial cells (mTECs) and T-cells. Dissection of thymus from mice for generation of purified T-cells and mTECs. Quantitative real time PCR analysis of progesterone-mediated changes of expression of RANK, RANKL, AIRE and FOXP3 in mTECs and T-Cells. Methods: qRT-PCR

2010 August - 2010 September, Internship

Center for Molecular Medicine of the Austrian Academy of Sciences

Group Stefan Kubicek

Project: "Set up of a high through put screening (HTS) assay for identification of inhibitors of methylated histone-binding-domains, related to AML". Cloning of vectors, subsequent protein expression in E.coli and purification. These proteins were histone-binding-domains which were used for following small molecule based HTS assays. Methods: Cloning, Protein expression

2008 October - 2009 June, Internship

Gregor Mendel Institute of Plant Biology

Group Karel Riha

1st Project: "Cloning for Yeast two Hybrid Assay, Identification of meiotic protein interactions"

2nd Project: "Optimization of Comet Assay – technique in Arabidopsis thaliana, Quantification of extra - chromosomal DNA fragments through In situ hybridization"

Technical Skills

| | |
|---------------------------|---|
| Working with cells | Flow cytometry, Cell membrane purification, viral infection of cells, cell-fusion assay |
| Organs and Tissues | In situ Hybridization on tissue sections Immunofluorescence staining and Confocal Microscopy |
| Proteins | Western blotting, Gel Electrophoresis (SDS - PAGE), Protein expression and purification |
| DNA and RNA | Isolation of DNA and RNA, PCR - Amplification, Cloning, Reverse Transcription, qRT – PCR |

Interests, Skills and Extracurricular Activities

| | |
|------------------|--|
| 2010 July | Volunteering, International AIDS Conference Vienna Session room Supervisor |
| 2002 July | Workcamp, Armenian Centre for International Co-operation (ACI) Spitak Organizing sportive activities, teaching English to children |
| Languages | Spanish (mother tongue) German, English and French (fluent) |
| Interests | Languages, Travelling, Sports, Music |

References

Magdalena Paolino, Ph.D.

Institute of Molecular Biotechnology (IMBA)

Group: Josef Penninger

Phone: +43 1 79044 - 4715

Magdalena.Paolino@imba.oeaw.ac.at

Stefan Kubicek, Ph.D.

Research Center for Molecular Medicine (CeMM)

Head of Chemical Screening and Platform Austria for Chemical Biology (PLACEBO)

Phone: +43 1 40160 70 036

skubicek@cemm.oeaw.ac.at

Vincenzo Di Bartolo, Ph.D.

Institut Pasteur (Paris - France)

Group: Andres Alcover (Lymphocyte cell biology unit)

Phone: +33 1 4061 36 55

vincenzo.di-bartolo@pasteur.fr

Zusammenfassung

Die Interaktion zwischen (SRC homology 2 (SH2)-domain-containing leukocyte protein of 76 kDa) SLP76 und (Hematopoietic progenitor kinase1) HPK1 ist essentiell für eine erst kürzlich entdeckte Negativ-Regulation der T-Zell-Aktivierung. Es wurde gezeigt, dass eine einzige Punktmutation in SLP76 (S376A), die Phosphorylierung dieses Proteins durch HPK1 verhindert und somit die Negativ-Regulation beeinträchtigt. Folglich, sind reagieren T-Zellen dieser Mutante sensitiver auf aktivierende Stimuli.

SLP76 ist eine Hauptkomponente einer sich, bei T-Zell Rezeptor Stimulation, bildenden Signaling-Plattform. Zahlreiche Prozesse können von SLP76-mediertem Signaling beeinflusst werden wie z.B.: Zell-Proliferation, -Survival, -Maturation und Differenzierung. SLP76 ist darüber hinaus bekanntlich essentiell für T-Zell Entwicklung.

Ein SLP76-S376A Mausmodell wurde generiert um die physiologische Relevanz dieser defekten Negativ-Regulierung zu überprüfen. Diese Arbeit ist eine Charakterisierung eines SLP76-S376A mutanten Mousmodells, mit Fokus auf frühe Signaling-Events, Downstream-Effektorfunktionen und auch T-Zell Entwicklung im Thymus.

In Übereinstimmung mit publizierten Daten für das HPK1 knock-out Mausmodell, demonstriert die SLP76-S376A Mutante keinerlei Defekte in T-Zell Entwicklung. Die SLP76-S376A Mutante zeigt jedoch, erhöhte Proliferationsraten und ERK (Extracellular signal-regulated kinase) Phosphorylierung in CD4+ und CD8+ SLP76-S376A T-Zellen, so wie auch inkrementierte INF- γ Produktion in SLP76-S376A CD8+ T-Zellen, im Vergleich zu Wildtyp T-Zellen.

Schlussendlich präsentiert die SLP76-S376A Mutante einen Satz veränderter T-Zell-Eigenschaften welche von einer defekten Negativ-Regulierung, der T-Zell Rezeptor Aktivierung, stammen. In einem HPK1 knock-out Mausmodell wurde erst kürzlich verstärkte, T-Zell abhängige, Anti-Tumorimmunaktivität demonstriert (Alzabin et al. 2010). Aus diesem Grund habe ich eine biolumineszente Tumorzelllinie entworfen, welche verwendet werden kann um die Rolle der HPK1-SLP76-Interaktion in Anti-Tumorimmunaktivität zu eruieren.